Identification and validation of a 7-genes prognostic signature for adult acute myeloid leukemia based on aging-related genes

Peng Ke[1,2,*], Qian Zhu[3,*], Ting Xu[1,2,*], Xiaofei Yang[1,2], Ying Wang[1,2], Huiying Qiu[1,2], Depei Wu[1,2], Xiebing Bao[1,2], Suning Chen[1,2]

[1]National Clinical Research Center for Hematologic Diseases, Jiangsu Institute of Hematology, The First Affiliated Hospital of Soochow University, Suzhou, China
[2]Institute of Blood and Marrow Transplantation, Collaborative Innovation Center of Hematology, Soochow University, Suzhou, China
[3]Soochow Hopes Hematonosis Hospital, Suzhou, China
*Equal contribution

Correspondence to: Xiebing Bao, Suning Chen; email: baosuyixueye@163.com, https://orcid.org/0000-0003-1628-5699; suning_chen0307@163.com, https://orcid.org/0000-0002-8298-4925

ABSTRACT

To explore effects of aging-related genes (ARGs) on the prognosis of Acute Myeloid Leukemia (AML), a seven-ARGs signature was developed and validated in AML patients. The numbers of seven-ARG sequences were selected to construct the survival prognostic signature in TCGA-LAML cohort, and two GEO datasets were used independently to verify the prognostic values of signature. According to seven-ARGs signature, patients were categorized into two subgroups. Patients with high-risk prognostic score were defined as HRPS-group/high-risk group, while others were set as LRPS-group/low-risk group. HRPS-group presented adverse overall survival (OS) than LRPS-group in TCGA-AML cohort (HR=3.39, P<0.001). In validation, the results emphasized a satisfactory discrimination in different time points, and confirmed the poor OS of HRPS-group both in GSE37642 (HR=1.96, P=0.001) and GSE106291 (HR=1.88, P<0.001). Many signal pathways, including immune- and tumor-related processes, especially NF-κB signaling, were highly enriched in HRPS-group. Coupled with high immune-inflamed infiltration, the HRPS-group was highly associated with the driver gene and oncogenic signaling pathway of TP53. Prediction of blockade therapy targeting immune checkpoint indicated varied benefits base on the different ARGs signature score, and the results of predicted drug response suggested that Pevonedistat, an inhibitor of NEDD8-activating enzyme, targeting NF-κB signaling, may have potential therapeutic value for HRPS-group. Compared with clinical factors alone, the signature had an independent value and more predictive power of AML prognosis. The 7-ARGs signature may help to guide clinical-decision making to predict drug response, and survival in AML patients.

INTRODUCTION

Acute myeloid leukemia (AML) is a type of malignancy that causes malignant clonal proliferation due to genetic mutations and seriously endangers human health [1], and it is far more common in elderly patients [2]. In the era of traditional chemotherapy, elderly AML patients face a significantly poorer prognosis, when compared with younger AML patients [3]. With the recent advent of molecularly targeted therapies, survival has been improved for elderly AML patients, but the prognosis is still poor [4, 5].

In elderly AML population, prognosis is associated with multiple factors. Badness of health status could lead to poor tolerance of the effective treatment measures [6].

Lower therapeutic response and shorter duration of remission time in the elderly patients may also result in irregular treatment [6, 7]. Moreover, elderly AML patients often accompany with multiple abnormalities both in cytogenetics and molecular biology [8].

Aging is a complicated, continual, progressive, and time-dependent biological process that results in decreased physiologic function across all organ systems, eventually culminating in death; it is an irreversible and progressive process [9], including genomic instability, metabolic changes, loss of ability for stem cell self-renewal, and so on [10]. It seems to be that aging is an adverse prognostic element for cancers, but the exact mechanism is still obscure [10, 11]. More frequency of mutations happened in epigenetic modifiers as AML patients got older [12]. On the other hand, aging could accelerate drastic decrease of B cell diversity, which may promote oncogenesis in the elderly patients [13]. Genetics and intrinsic factors play important roles in influencing aging. With the development of genomics and transcriptome sequencing, as well as the application of high-throughput genetic screens, over 300 genes have been found to be involved in aging in humans alone [14].

Not only targeted therapy but survival prediction could be guided by signatures of aging-related genes (ARGs) in multiple different tumors [15–18]. Moreover, the primary markers of aging such as ARGs have been investigated widely, and the most main phenotypes contained mitochondrial dysfunction and immunological senescence [19]. To evaluate the effects of ARGs on prognosis of adult AML, we obtained ARGs from website of HAGR (human aging genome resource) [20] and assessed the association between ARGs and AML prognosis.

RESULTS

Construction of ARGs-related prognostic signature

The flow chart of this study was presented in Supplementary Figure 1. In training set (TCGA-LAML, n = 151), 83 (55.0%) were male and 68 (45.0%) were female, with a median age of 56 years at diagnosis. In patients with complete survival data (n = 140), the median time of OS was 577 days.

Univariate COX analysis demonstrated that 84 of 307 ARGs were associated with AML prognosis (Supplementary Figure 2). Via random survival forest algorithm (Figure 1A, 1B), we identified a 7-ARGs signature with a lowest OOB error rate for predicting AML survival (Figure 1C), Subsequently, seven ARGs with a relative importance greater than 0.52 were transferred to establish a prognostic signature for AML

(Figure 1D). Table 1 described the coefficients and other parameters of these seven ARGs in detail. The Prognostic Risk Score (PRS) of signature was estimated as follows:

$$\begin{aligned} PRS = {}& 0.466051 \times PTPN1 + 0.430832 \times DGAT1 \\ & + 0.377577 \times SOD1 + 0.250209 \times GSTP1 \\ & + 0.050049 \times NUDT1 - 0.001312 \times EMD \\ & - 0.443539 \times STK11 \end{aligned}$$

Validation of 7-ARGs prognostic signature

In training set, patients were divided into HRPS- and LRPS-group according to median value of PRS (Figure 2A). LRPS-group had a notably better OS than HRPS-group (Figure 2B, *P*<0.001). The median survival time of LRPS-group was 915 days (Q1: 303.75, Q3: 1193.5), whereas that of HRPS-group was 242 days (Q1: 52, Q3: 372.75). The area under curves (AUCs) meant that 7-ARGs signature has a good predictive performance (Figure 2C), with values of 0.780, 0.772 and 0.691 at 1- , 2-, and 3-year.

Then, two independent datasets were applied to verify the performance of this 7-ARGs signature. Patients in GSE37642 were stratified into two different risk groups in terms of the median PRS value too (Figure 2D). Similarly, LRPS-group significantly prolonged OS (Figure 2E, *P*=0.001), and 7-ARGs signature also had an ability to predict OS (Figure 2F). In GSE106291 cohort (Figure 2G), HRPS-group exhibited a worse OS than LRPS-group (Figure 2H, *P*<0.001), and values of AUCs at 1-, 2- and 3-year were 0.639, 0.654 and 0.641 (Figure 2I).

GSEA analysis

GSEA analysis of KEGG connoted that HRPS-group was enriched in many pathways, such as signaling of *WNT*, Toll-like receptor and *MAPK*. Similarly, many items of immune pathways were also enriched in HRPS-group (processing and presentation of antigen, interaction of cytokine and cytokine receptor, signaling pathway of Chemokine and T cell receptor) (Figure 3A).

The results of hallmark analysis suggested that many tumor-related signaling pathways were identified for HRPS-group (Figure 3B), such as *NF-κB* pathway in response to *TNF*, *IL-25* signaling pathway through *STAT5*, signaling pathway of *IL6/JAK/STAT3*, *p53*, *KRAS*, *notch*, and *TGF-β*.

Characteristics of immune-related cells

The assessments above confirmed the prognostic value and biological function of the 7 ARGs-related

signature, including many tumors and immune/inflammatory signaling pathways, prompting us to further explore the different proportion of immune-related cells between HRPS- and LRPS-group. HRPS-group had a higher ESTIMATE and immune score than LRPS-group (Supplementary Figure 3). The differences of immune-related features were displayed in Figure 4, and the results were almost consistent with each other in three AML cohorts (TCGA-AML, GSE37642 and GSE106291). HRPS-group were accompanied with higher scores of immune cells, such as MDSCs (myeloid-derived suppressor cells), many subtypes of T cell (central memory CD8 T, regulatory T, and Gamma delta T), Monocyte,

macrophage, and etc. In addition, HRPS-group was characterized by increased enrichment of MHC I, Parainflammation, Type-I *IFN* Response and Check-point (Supplementary Figure 4).

Immune checkpoints play an important role in regulating immune infiltration [21], and up-regulated score of check-point molecule in HRPS-group might be a potential therapeutic target. So, we next explored the relevance of PRS and expression levels of 8 immune checkpoints, which indicated that *PDCD1* (R= 0.314), *LAG3* (R= 0.247), *CTLA4* (R= 0.199), and *CD274* (R= 0.198) had a positive relationship with PRS (Supplementary Figure 5).
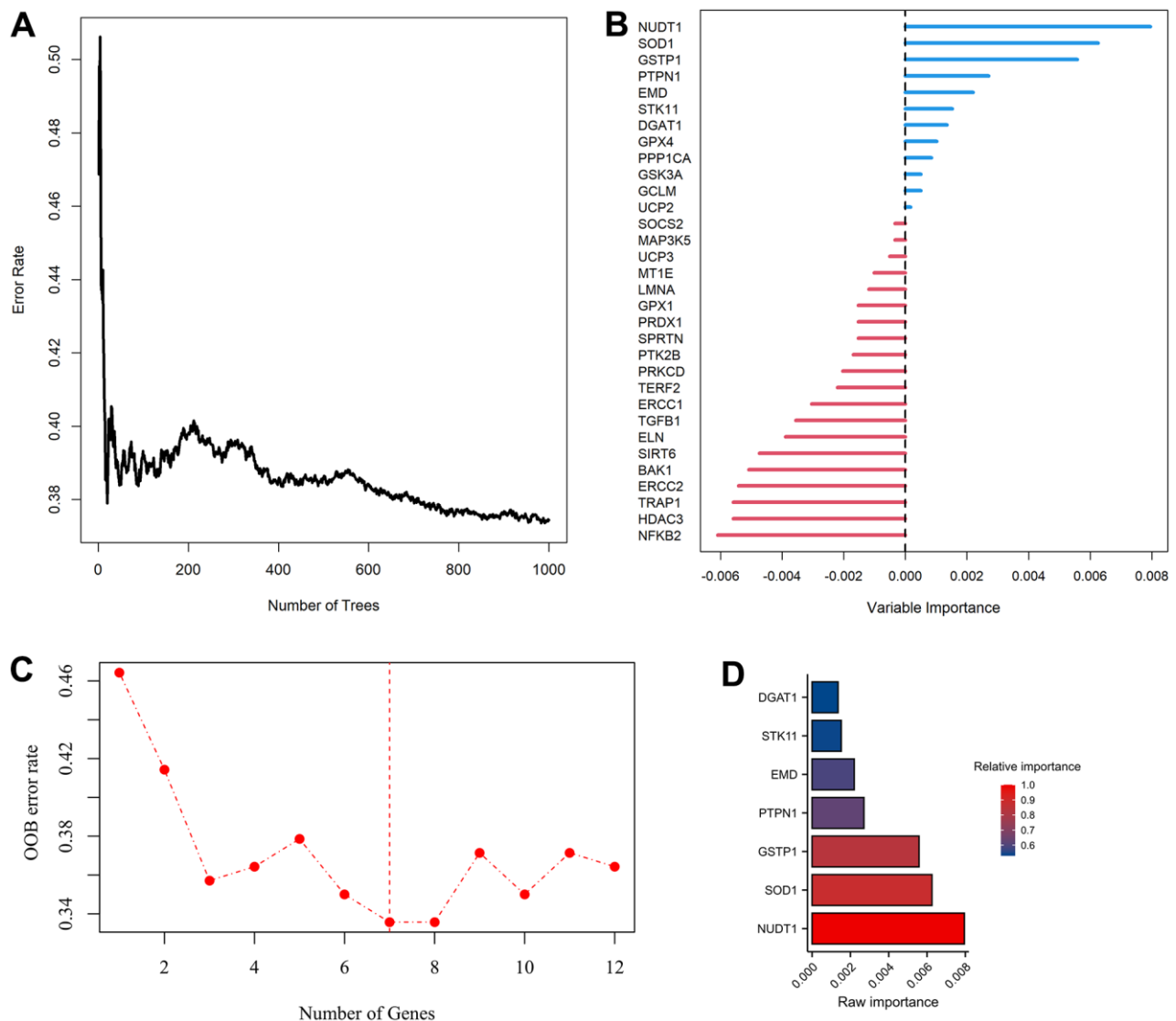
Figure 1. Modelling of aging-related genes (ARGs) prognostic signature. (**A**) Random survival forest algorithm for selecting hub ARGs. (**B**) The raw importance of the 32 candidate ARGs. (**C**) Weighted random forest (Ranger) was preformed to choose the optimization model with a lowest out of bag (OOB) error rate. (**D**) Seven ARGs with a relative importance greater than 0.52 were transferred to construct prognostic signature using COX regression model.

Table 1. Multivariate COX regression analysis of 7 prognosis-related ARGs in AML.

Ensemble gene ID	Symbol	Coefficient	Hazard ratio	Importance	Relative importance
ENSG00000196396	PTPN1	0.466051	1.593688	0.008	1.000
ENSG00000185000	DGAT1	0.430832	1.538536	0.006	0.880
ENSG00000142168	SOD1	0.377577	1.458746	0.006	0.831
ENSG00000084207	GSTP1	0.250209	1.284294	0.003	0.627
ENSG00000106268	NUDT1	0.050049	1.051322	0.002	0.590
ENSG00000102119	EMD	-0.001312	0.998689	0.002	0.542
ENSG00000118046	STK11	-0.443539	0.641761	0.001	0.530

Abbreviations: ARGs, aging-related genes; AML, Acute Myelocytic Leukemia.

Scores of twelve subtypes in ARGs signal

To explore the distribution of ARGs subtypes and possible pathogenic mechanisms between HRPS- and LRPS-group, ssGSEA was performed to assess each score of 12 aging-related gene subsets. Results manifested that score of altered intercellular communication, deregulated nutrient sensing, *NF-κB* related gene and others were remarkably increased in the HRPS-group; whereas the score of stem cell exhaustion and genomic instability depressed inversely (Supplementary Figure 6).

Mutation profile between HRPS- and LRPS-group

The top 20 frequent genes of mutation were visualized in Figure 5. *NPM1* was the primary mutated gene in LRPS-group (Figure 5A), whereas *TP53*, *KIT* and *FLT3* mutated frequently in HRPS-group (Figure 5B). The results of Oncogenic Signaling Pathways revealed that LRPS-group displayed a higher frequency of mutations, which were enriched in many different pathways, including *NRF2*, *TGF-β*, *Hippo*, *MYC*, *PI3K* and Cell Cycle (Figure 5C). In HRPS group, *TP53* followed by *RAS* and *NOTCH* pathways were the most mutation-enriched pathways (Figure 5D). Forest plot confirmed that HRPS-group occurred more frequent *TP53* mutation (Figure 5E). However, no difference of TMB was found between these two groups (Figure 5F). PRS distributions showed that more patients with higher PRS were assigned to *FLT3-TKD* mutation (Supplementary Figure 7A), but those with lower PRS were more likely to appear in mutations of double *CEBPA* and *IDH2* (Supplementary Figure 7B, 7C). However, no differences of PRS distribution were found between patients with wild type and mutations of *FLT3-ITD, NPM1, IDH1*, *KRAS*, and *NRAS* (Supplementary Figure 7D–7H). These results implied that HRPS-group was highly associated with the driver gene and signaling pathway of *TP53*.

High PRS patients may response to Pevonedistat

The predicted response hinted that increased PRS was significantly correlated with decreased score of TIDE (Figure 6A, *P*=0.023) and increased dysfunction score (Figure 6B, *P*=0.005). No difference of TIDE score was seen between these two groups, while HRPS-group had a higher dysfunction score (Figure 6D, *P*<0.001). In addition, a markedly lower IC50 value of Pevonedistat was found in HRPS-group (Figure 6E, *P*<0.001), and other information of predicted drugs with potential therapeutic values could be downloaded in Supplementary Tables 7, 8. A negative and moderate correlation was also seen between IC50 level of Pevonedistat and PRS (Figure 6F, *P*<0.001).

Pevonedistat is an inhibitor of *NEDD8*-activating enzyme, the response of which is significantly correlated with expression level of *NEDD8*. To reveal the relationship between 7-ARGs signature and *NEDD8* expression level, Figure 6G demonstrated that *NEDD8* expression is positively related with PRS (R=0.457), and negatively (Figure 6H, R= -0.647) related with the predicted IC50 of Pevonedistat (*P*<0.001). Moreover, HRPS-group also had a higher *NEDD8* expression than LRPS-group (Figure 6I, *P*<0.001). These results suggested that Pevonedistat may be a potential drug for the HRPS-group.

Development of a nomogram containing 7-ARGs signature

The clinical features of TCGA-LAML were described in Table 2. No significant differences were found between HRPS- and LRPS-group, including gender, race, gene mutation of *FLT3*, *RAS*, *NPM1* and *IDH1*. However, adverse-risk of cytogenetics and older patients were occurred frequently in HRPS-group (P<0.05).

To seek clinical applicability, we constructed a predicted Nomogram composed of 7-ARGs signature in training

set. Results of univariate and multivariable survival analysis could be found in Supplementary Table 9 and Figure 7A. All predictors accompanied with a VIF value less than 5, which meant that no collinearity happened in the predicted nomogram. Combining with age, cytogenetics risk and PRS of ARGs signature, a nomogram was constructed for predicting AML prognosis (Figure 7B). According to the nomogram, the cytogenetics risk stratification can be further reclassified (Figure 7C), and prognostic difference of OS was well accounted too (Figure 7D, *P*<0.001). Good performance was verified by calibration plots (Figure 7E).
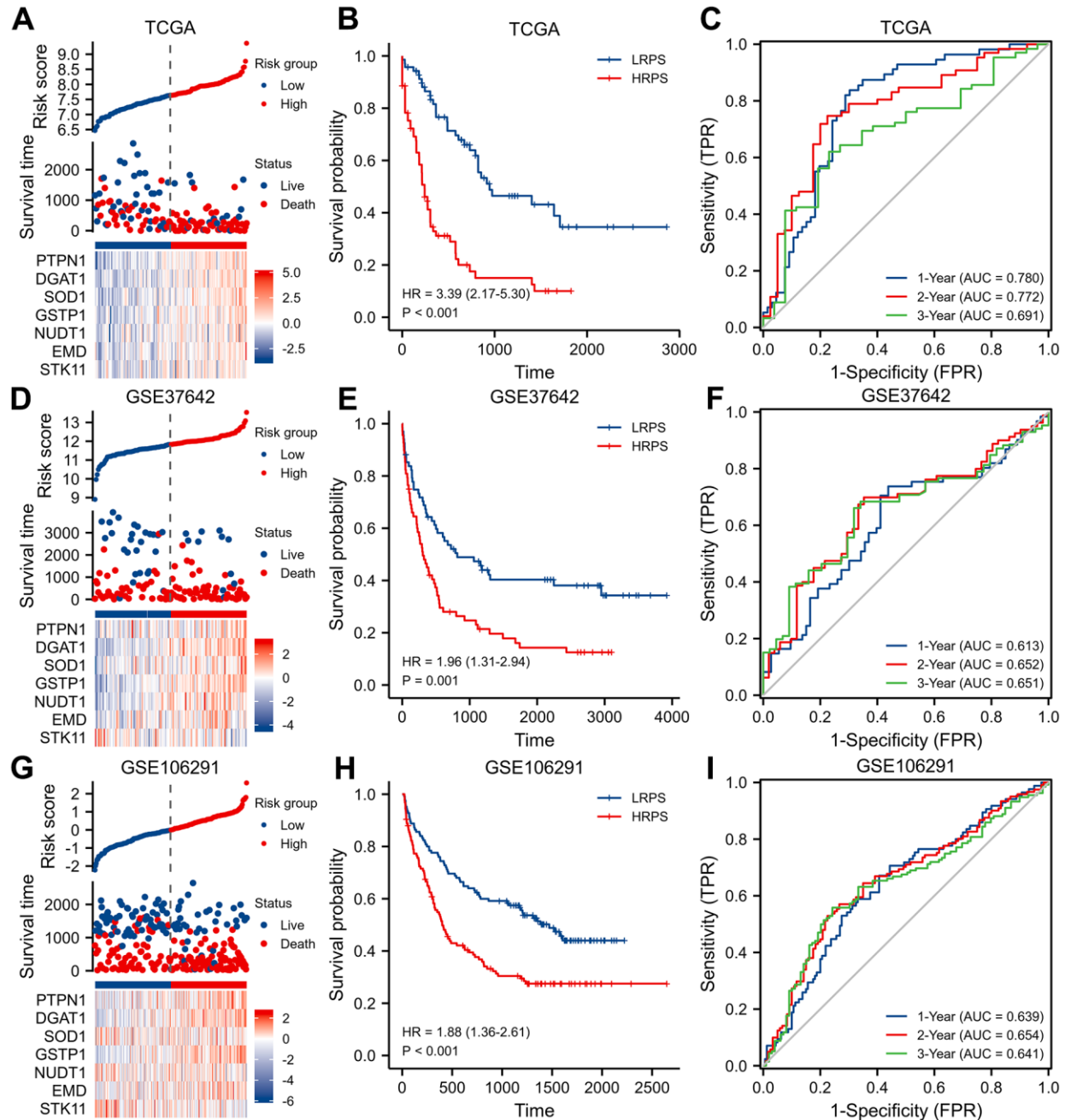

Figure 2. Identification and validation of a seven-ARGs prognostic model. (**A**) Plot of risk classification, survival status and heatmap of seven-ARGs; (**B**) curve of OS (Overall Survival) stratified by high-risk prognostic score (HRPS)-group/high-risk group and low-risk prognostic score (LRPS)-group/low-risk group; (**C**) curves of time-dependent ROC (receiver operator characteristic) in training set. (**D**–**F**) Plot of risk classification, survival status and heatmap of seven-ARGs; curve of OS; curves of time-dependent ROC in validation set of GSE37642. (**G**–**I**) Plot of risk classification, survival status and heatmap of seven-ARGs; curve of OS; curves of time-dependent ROC in validation set of GSE106291.

Moreover, plots of C-statistic demonstrated a good discrimination (Figure 7F), with a value of 0.754, 0.741 and 0.731 at 1-, 2- and 3-year, respectively. Compared with the model of age or combined model with age plus cytogenetics risk, higher C-statistic values were seen in predicted nomogram (Figure 7F). With regard to DCA analysis at 1-, 2- and 3-year, various degrees of benefits were presented for nomogram prediction than two other models. Moreover, using the nomogram to predict AML prognosis could add more benefits than either the strategy of intervene-none or intervene-all-patients if the probability is higher than the threshold (Figure 7G–7I).

DISCUSSION

AML is a common malignant tumor in the elderly [2], and these group of patients were associated with poor prognosis [22–24]. However, the mechanism how aging affects AML prognosis is not quite clear. A prognostic signature base on expression level of 7-ARGs was established and verified in this study, which can well classify AML patients into two risk groups with different prognosis.

In the 7-ARGs signature, *PTPN1*, *DGAT1*, *SOD1*, *GSTP1*, and *NUDT1* acted as risk factors, whereas *EMD* and *STK11* were protective factors. Some of them were confirmed with the formation and progression of AML. Overexpression of *GSTP1* is linked with drug resistance in AML [22]. *STK11* is a tumor suppressor gene, which can encode kinase B1 in liver (*LKB1*) [23], and pathway regulated by which was highly associated with tumor suppression in AML [24]. Although there are no definite investigations of the roles other five ARGs played in AML, these genes will be worthy of further study. The 7-ARGs signature exhibited a good performance in predicting overall survival both in the training and validation cohorts. Adjusted by clinical features, 7-ARGs signature acted as an independent risk factor of AML prognosis. Furthermore, the nomogram based on
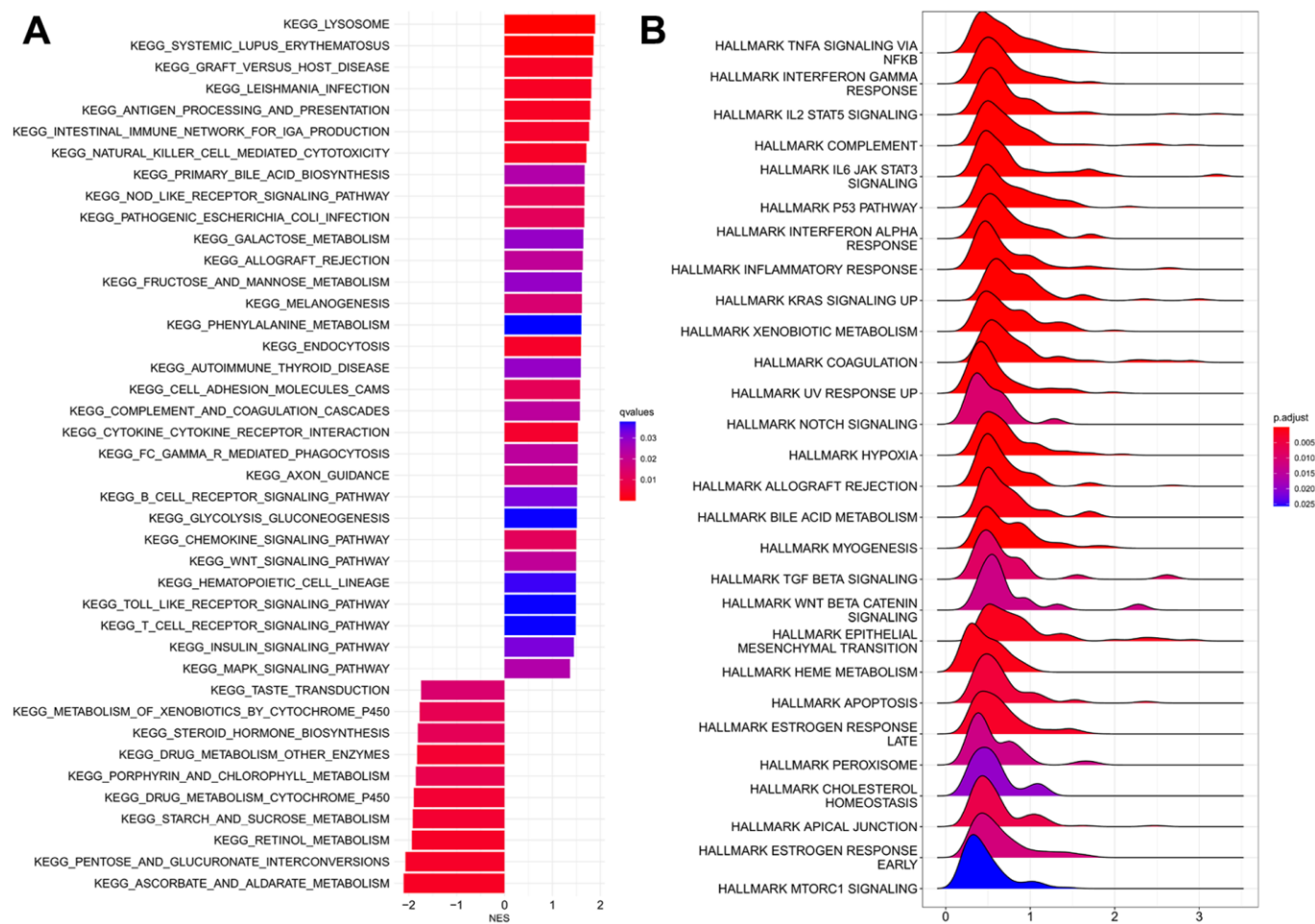

Figure 3. GSEA analyses between HRPS-group/high-risk group and LRPS-group/low-risk group. (**A**) KEGG analyses. (**B**) Analyses of hallmark pathways.

7-ARGs signature both took on a good calibration and discrimination, which can also help to make clinical decisions.

Functional analyses of 7-ARGs signature emphasized that HRPS-group was enriched in pathways of processing and presentation of antigen, interaction of cytokine receptor, and Toll-like receptor, which could help to promote AML progression [25]. Activation of inflammatory pathways can also lead to myeloproliferative disease by increasing levels of cytokine and ROS (reactive oxygen species) [26].
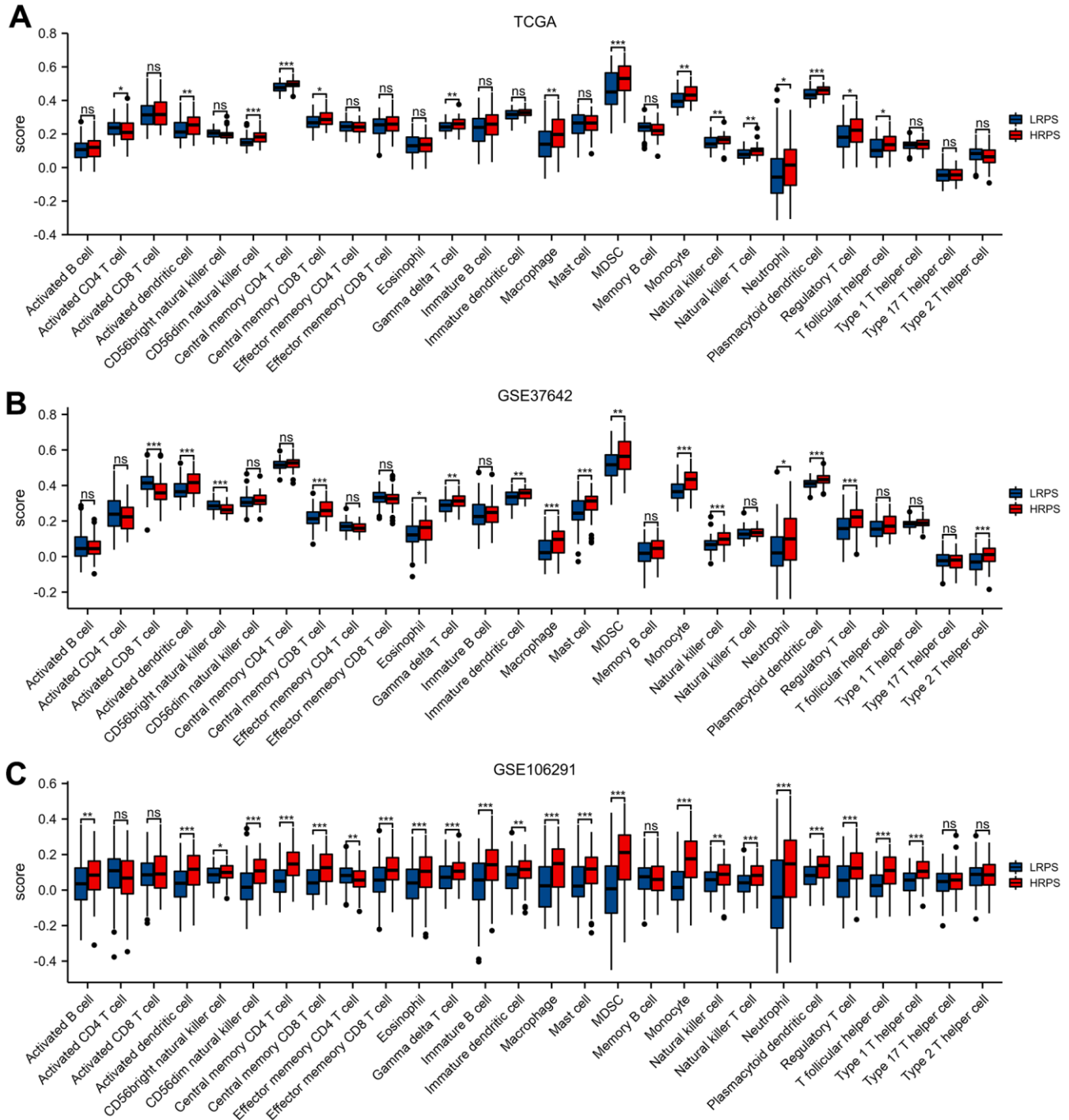
Figure 4. Different cell abundance of twenty-eight immune categories between HRPS-group/high-risk group and LRPS-group/low-risk group in training set (**A**) and validation set (**B**, **C**). (*P < 0.05, **P <0.01, ***P < 0.001).
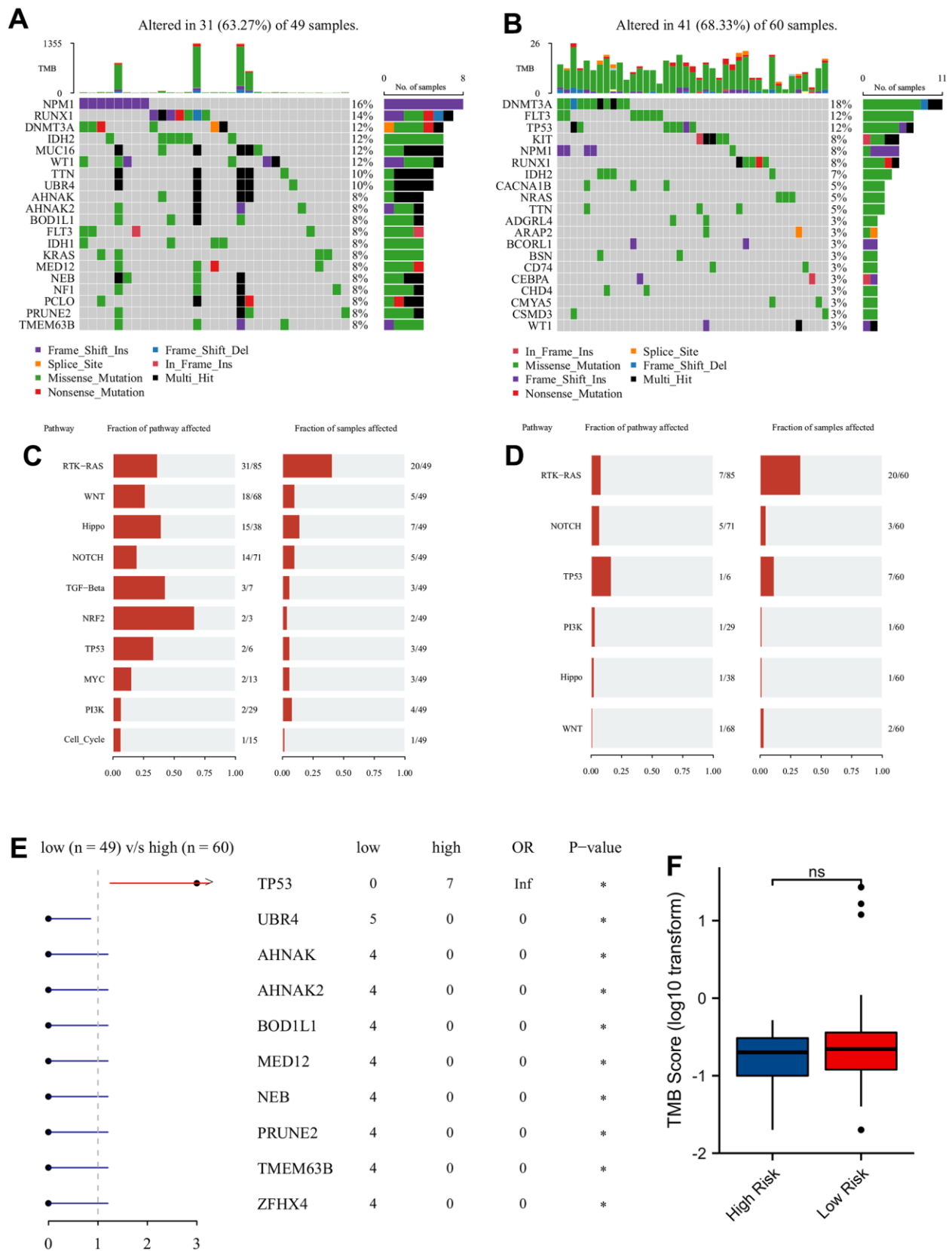
Figure 5. Mutation analysis of two different prognostic risk score groups. Oncoplot of top 20 high frequency of mutated genes in LRPS-group/low-risk group (**A**) and HRPS-group/high-risk group (**B**). The major mutation-enriched pathways in LRPS-group/low-risk group (**C**) and HRPS-group/high-risk group (**D**). Difference of mutated genes (**E**) and TMB score (**F**) in two different PRS groups.

GSEA analysis revealed that signaling pathways of *NF-κB* and *KRAS* were significantly activated in HRPS-group. AS a member of transcription factors, *NF-κB* is widely involved in many biological processes, such as responses of immune and inflammation, proliferation, differentiation, cell survival, and all of which were strongly linked to survival of AML stem cells [27–31]. Results *in vivo* and *vitro* also verified that inhibiting
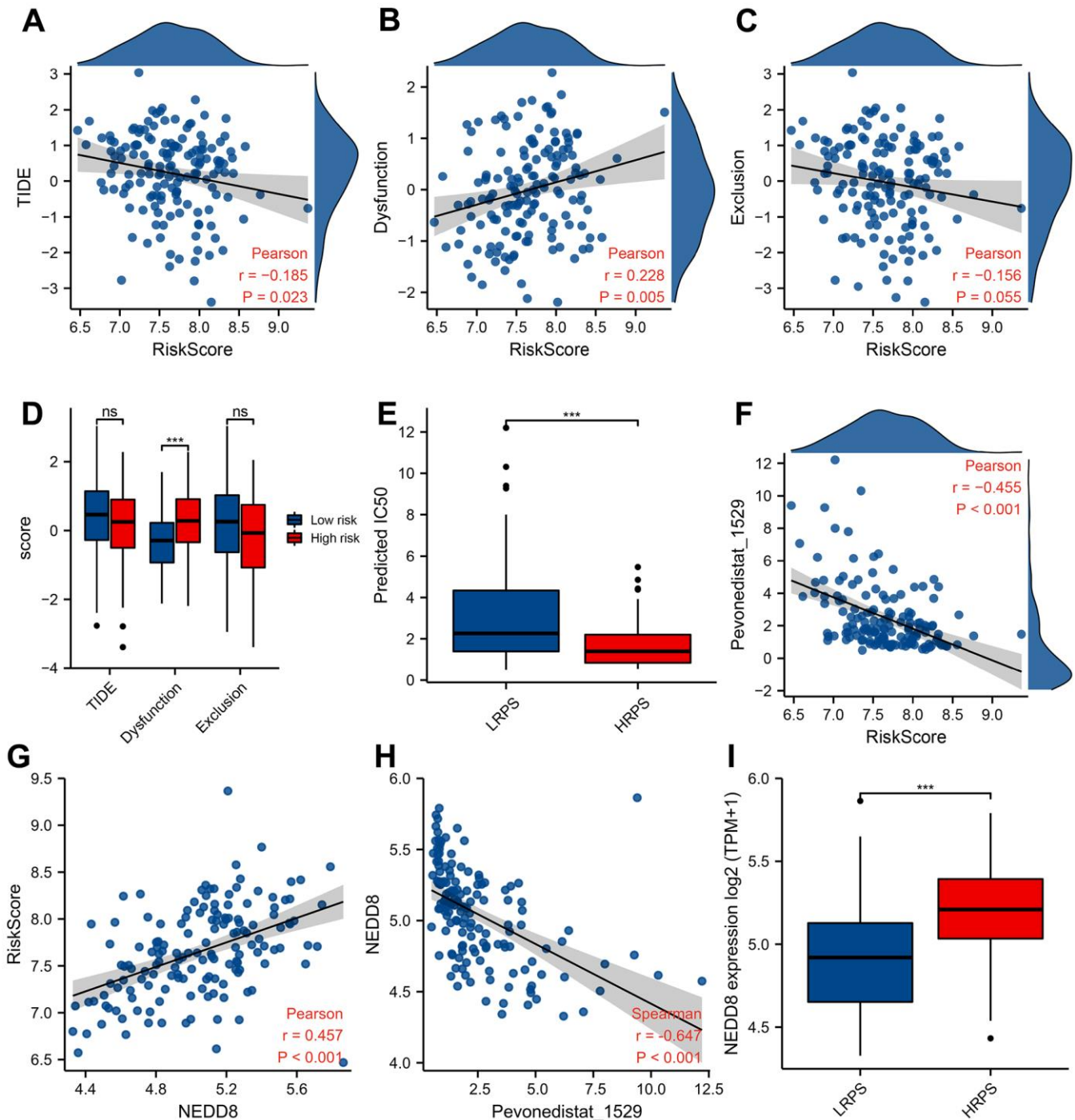
Figure 6. Predictive response of checkpoint blocking-up and drug in training cohort. Correlation between PRS and TIDE score (**A**), Dysfunction score (**B**), and Exclusion score (**C**). Boxplot of TIDE/Dysfunction/Exclusion score (**D**) and IC50 value of Pevonedistat (**E**) in HRPS-group/high-risk group and LRPS-group/low-risk group. (**F**) Relationship between Pevonedistat IC50 and PRS according to 7-ARGs signature, and an outlier was removed from curve of Pearson correlation analysis. Correlation analysis of PRS (**G**) and Pevonedistat's IC50 (**H**) with the *NEDD8* expression level. Boxplot of *NEDD8* expression level in HRPS-group/high-risk group and LRPS-group/low-risk group (**I**).

Table 2. The characteristics of 151 acute myeloid leukemia patients in TCGA database.

Characteristic	Low-risk (n=76)	High-risk (n=75)	P value
Gender			0.284
Female	38 (25.2%)	30 (19.9%)	
Male	38 (25.2%)	45 (29.8%)	
Race			1.000
Asian or unavailable	2 (1.3%)	1 (0.7%)	
Black or African American	7 (4.6%)	6 (4.0%)	
White	67 (44.4%)	68 (45.0%)	
Age (Median [IQR]) years	51 [35.8, 62.0]	62 [47.5, 69.5]	0.001
Cytogenetics risk			0.004
Favorable	22 (14.8%)	9 (6.0%)	
Intermediate	43 (28.9%)	39 (26.2%)	
Adverse	11 (7.4%)	25 (16.8%)	
FLT3 mutation			0.956
Negative	52 (35.4%)	50 (34.0%)	
Positive	22 (15.0%)	23 (15.6%)	
RAS mutation			0.719
Negative	71 (47.3%)	71 (47.3%)	
Positive	5 (3.3%)	3 (2.0%)	
NPM1 mutation			1.000
Negative	59 (39.3%)	58 (38.7%)	
Positive	17 (11.3%)	16 (10.7%)	
IDH1 mutation			0.593
Negative	61 (40.9%)	62 (41.6%)	
Positive	15 (10.1%)	11 (7.4%)	
PB-blast (%)	70 [51.0, 85.0]	73 [48.0, 85.0]	0.994
BM-blast (%)	45.5 [12.5, 70.3]	23 [6.0, 56.0]	0.065
WBC ($\times 10^9$/L)	14.5 [4.0, 42.3]	26.5 [6.0, 61.3]	0.214
Hemoglobin (g/L)	90 [60, 130]	90 [60, 130]	0.940
PLT ($\times 10^9$/L)	45.5 [27.3, 87.3]	44 [30.5, 83.5]	0.669

Abbreviations: TCGA, The Cancer Genome Atlas; IQR, Interquartile range; FLT3, FMS-like tyrosine kinase 3; NPM1, Nucleophosmin; IDH1, Isocitrate dehydrogenase 1; PB, Peripheral blood; BM, Bone marrow; WBC, White blood cell; PLT, Platelet.

pathway of *NF-κB* could provoke cell death in AML, while this phenomenon was not obvious in normal bone marrow stem cells [31, 32]. Moreover, abnormal activation of *NF-κB* signal has been proven to involve in the process of AML resistance to chemotherapeutic agents [33]. In addition, excessive activation of *RAS* signaling is also considered to be one of the primary pathogenic items of AML [34]. All these may help to account for poor prognosis of AML patients in HRPS-group.

Aging changed the status of immunity and microenvironment as always, which might also facilitate tumor progression [35]. Our results certified that HRPS-group had significantly a higher score of ESTIMATE and immunity. Consistent with previous studies [36], our results suggested that higher immune score could also lead to adverse prognosis. HRPS-group had more increased components of immune suppression by myeloid cells, monocyte and macrophage, which could also lead to a poor survival rate. TAMs (tumor-associated macrophages) could promote leukemic stem cells proliferation and immortality via diverse mechanisms, including angiogenesis, extracellular matrix remodeling, and lymphangiogenesis [37, 38]. Immune suppression by myeloid cells, one of MDSCs, could also block the anti-tumor effects by multiple mechanisms, which may also help to explain to some

extent why HRPS-group was accompanied with poor prognosis [39].

The aging process affects not only immune system by enhance or suppress of immune cell function, but also immune supervision of checkpoints [40, 41]. Nowadays, therapy of blocking checkpoint has led to breakthroughs in cancer therapy, such as lymphomas, lung cancer and melanoma [42]. Although studies of immune checkpoint therapy in AML were limited, some studies still had encouraging results [42–44]. It is of great significance to find reliable predictive biomarkers and therapeutic targets for AML with different risks. Positive correlations were found between PRS from ARGs signature and four expression genes of checkpoints (*PDCD1*, *CTLA4*, *LAG3* and *CD274*). TIDE algorithm also revealed that higher 7-ARGs signature score was highly in relation to lower TIDE
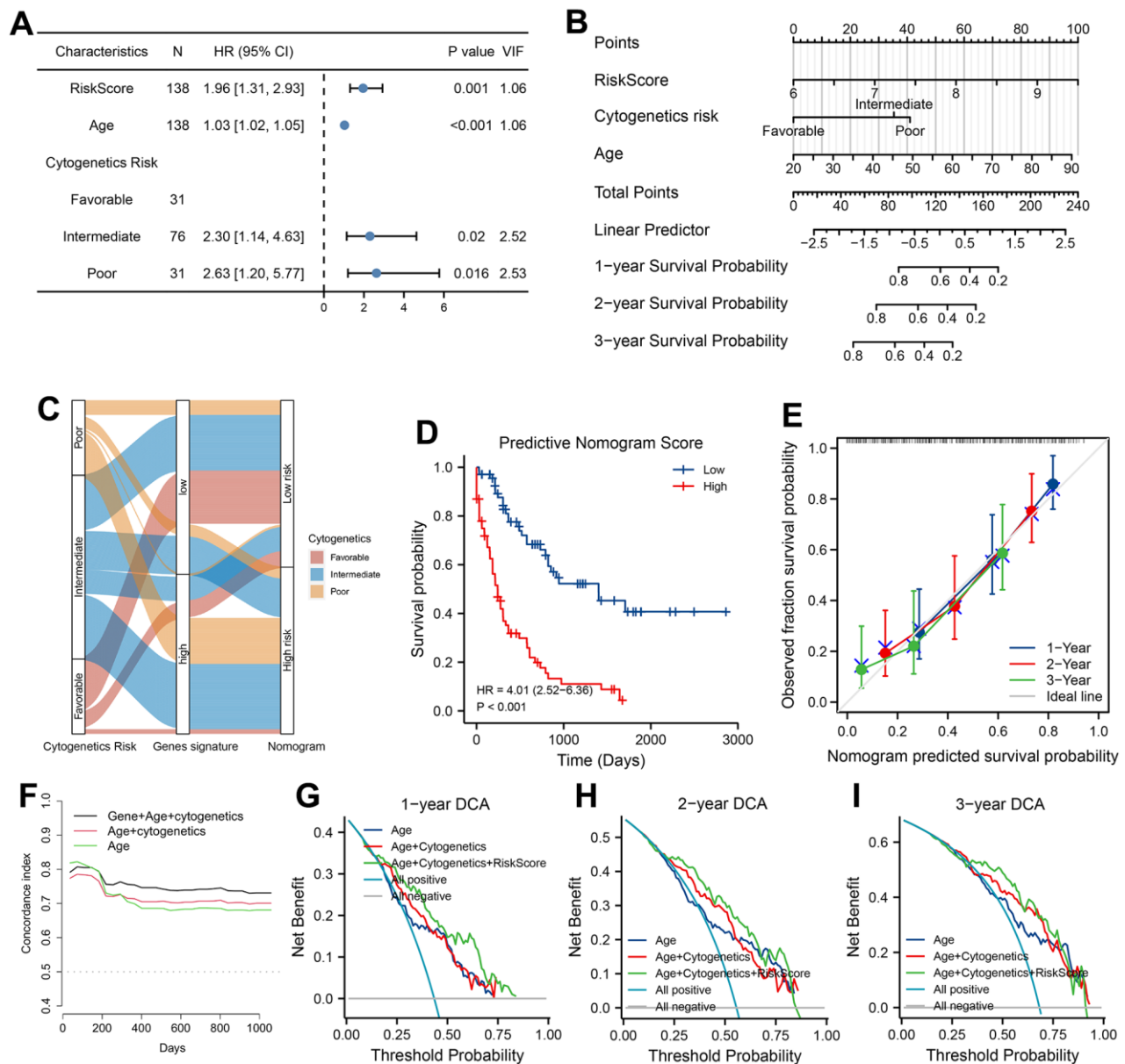
Figure 7. Development, validation and clinical use of predicted nomogram. (**A**) Prognostic analysis of Nomogram. VIF indicated Variance inflation factor. (**B**)Construction of Nomogram according to prognostic factors of AML patients in training cohort. Values of prognostic risk Score (PRS) were calculated by 7-ARGs signature. (**C**) Sankey diagram of transitions from cytogenetics risk category to reclassification of 7-ARGs signature and Nomogram. (**D**) Analysis of survival relying on stratification of Nomogram. (**E**) Calibration curve of Nomogram at 1-, 2-, and 3-year. Discrimination with C-statistic at different time (**F**) and DCA plot at 1-, 2- and 3-year (**G**–**I**) for Nomogram and clinical features (model with age alone or with age plus cytogenetics risk).

score, and lower TIDE score denoted more benefits from immune checkpoint therapy. No difference of TIDE score between two risk groups may due to higher dysfunction of T cells in HRPS-group, which may limit benefits of immune checkpoint therapy. Furthermore, Pevonedistat was predicted as a potential therapeutic drug for patients in HRPS-group. In 7-ARGs signature, *NF-κB* was the primary signaling with abnormal activation in HRPS-group, while Pevonedistat can inhibit *NF-κB* signaling [45], those might help to explain our results of drug prediction. Pevonedistat may be more suitable for AML with higher prognostic score of 7-ARGs signature.

Interestingly, subtype analysis of ARGs illustrated a consistent result with enrichment analysis. HRPS-group had a higher score of ssGSEA in *NF-κB* related gene set, which was the primary enrichment pathway in GSEA analysis. Furthermore, deregulated nutrient sensing were significant associated with humans' longevity [46]. Inflammation is one of the prominent alterations in aging-associated communication of intercellular space. This immunosenescence may affect the normal function of the body, dysfunction of clearing abnormal and/or infected cells, especially for tumor cells [10]. This suggests that altered intercellular communication may participate in modulating tumor development. Higher scores both in purity of tumor and genomic instability in LRPS-group may explain why this group of patients had a higher ssGSEA score of stem cell exhaustion. In addition, patients in HRPS-group had more frequent mutation of *TP53,* which was confirmed with poor prognosis in AML patients [47]. Accordingly, LRPS-group had a higher frequency of mutation in *UBR4*, *AHNAK*, *BOD1L1*, and etc. In Bladder Cancer, mutation of *AHNAK* is one sign of favorable prognosis [48]. Some of them, including *MED12*, *NEB*, and *ZFHX4*, were considered to be poor prognostic factors in some solid tumors [49–51], but the role of which in AML is unclear.

However, our current study also had some limitations. Firstly, although the effectiveness of 7-ARGs prognostic signature has been proved both in training and validation datasets, the applied AUC of validation set is unsatisfactory, which might be on account of different sequencing platforms. The training cohort is obtained from RNA-sequencing, while the validation set (GSE37642) is generated from microarray platform. Although the AUC values of validation cohorts are lower than that of the training set, predictive power is still exhibited in validation sets according to the curves of ROC and Kaplan-Meier survival analysis. Secondary, more independent cohorts and experimental studies (*in vitro* or *in vivo*) are required to validate the effectiveness and disclose underlying mechanisms. In

the future, the exact prognostic values of these ARGs deserve further study in AML.

CONCLUSIONS

In conclusion, we identified and validated an aging-related risk signature based on seven-ARGs for predicting AML prognosis, and also tried to reveal the possible mechanisms from many aspects. These findings could be helpful to improve diagnosis, risk stratification or treatment of AML.

MATERIALS AND METHODS

Source of data

TCGA-LAML cohort was downloaded as the training set for constructing prognostic signature base on ARGs, including publicly available gene expression and clinical data. The RNA-seq data of which was standardized by Transcripts Per Kilobase of exon model per Million mapped reads (TPM) and normalized as log2 (TPM + 1). Two independent AML datasets of GEO, including GSE37642 (GPL570 platform, n = 136) and GSE106291 (n = 250), were also adopted to validate the reliability of prognostic signature. Human ARGs were obtained from the website of HAGR (Supplementary Table 1, n = 307) (https://www.genomics.senescence.info/). Moreover, GSE14468 (n = 461) was also acquired to further compare the differences of PRS between several gene mutations, including *NPM1*, *IDH1*, *IDH2*, *KRAS*, *NRAS*, *CEBPA*, *FLT3-ITD*, and *FLT3-TKD*. All data used in this study were conducted in accordance with the publication guidelines, as a result, informed consent and ethical approval were not required.

Development and validation of a 7-ARGs signature for AML prognosis

According to the median value of gene expression, univariate COX analysis was carried out to select ARGs with prognostic values in the training set (Supplementary Table 2). A total of 48 ARGs were associated with AML prognosis (Supplementary Table 3, *P*<0.05), with 35 of adverse prognostic ARGs and 13 of favorable prognostic ARGs. Thirty-two of 35 adverse prognostic ARGs were chosen as candidate genes, which were co-expressed in GSE37642 cohort. The importance of 32 ARGs was ranked using a model of random survival forest (ntree=1000, "randomForestSRC" R package) [20]. To choose the optimal model for constructing prognostic signature, 12 of 32 ARGs with a positive raw importance were chosen and screened using method of weighted random forest ("Ranger", "randomForest" and "survival" R packages). Finally, seven-ARGs signature was identified with a lowest out of bag (OOB) error rate

in the training set, and seven ARGs with a relative importance greater than 0.52 were transferred to further assessment using by COX regression model. The expression level and COX regression coefficient of ARGs were used to calculate the prognostic risk score (PRS) as below:

$$\text{Prognostic risk score (PRS)} = \sum_{i=1}^{n} \text{Coef}(i)\,X(i)$$

where n indicates the number of ARGs included in the prognostic signature, Coef(i) means the coefficient of each ARGs in COX regression, and X(i) represents the expression level of each ARGs. In the light of median PRS value, AML patients were categorized into two subgroups. Patients with high value of PRS were defined as HRPS-group/high-risk group, while others were deemed as LRPS-group/low-risk group. Curves of survival analysis and time-dependent ROC analysis were performed to evaluate the survival differences and discrimination of ARGs signature, using R packages of "survival", "ggrisk", "survminer" and "timeROC".

Enrichment analyses

To assess biological functions and signaling pathways associated with HRPS-group, gene set enrichment analysis (GSEA) was carried out using programs of Hallmark and c2 KEGG from MSigDB. The significant difference was set as |normalized enrichment score| >1, False Discovery Rate < 0.25, and the adjusted *P* value lower than 0.05.

Immune characteristics of microenvironment

Differences of immune-related characteristics were analyzed between the HRPS- and LRPS-group, adopting R package of ESTIMATE for calculating stromal-score, immune-related score, purity of tumor, and ESTIMATE-related score [52]. Meanwhile, using R packages of GSVA and GSEABase, ssGSEA was performed to quantify different types of immune-related cells. The immune-related gene sets were collected from previous studies (Supplementary Tables 4, 5) [53, 54]. To further identify the potential therapeutic targets of checkpoints for ARGs signature, we also evaluated the correlations of PRS with the expressed levels of 8 immune-related checkpoints (*HAVCR2*, *SIGLEC15*, *PDCD1*, *PDCD1LG2*, *CD274*, *LAG3*, *CTLA4* and *TIGIT*).

ssGSEA analysis of twelve aging-related gene signals

According to previous studies [55], all ARGs can be divided into 12 sub-categories, which may help to

conceptualize the essence of cancers and their underlying mechanisms. To depict the distributions of different subtypes and possible pathogenic mechanisms between these two different risk groups, ssGSEA was also performed in 12 aging-related gene sets from National Genomics Data Center (Supplementary Table 6, https://ngdc.cncb.ac.cn), including *NF-κB* related gene, senescence-associated secretory phenotype, stem cell exhaustion, telomere attrition and others. We compared the difference of 12 ssGSEA scores between the HRPS- and LRPS-group.

Mutational features

To better understand the difference of driver genes between HRPS- and LRPS-group, the somatic mutations of TCGA-LAML were acquired and analyzed using R package of "maftools" [56]. The mutational landscape of two different PRS groups were investigated by Fisher exact test, and visualized graphically using by waterfall curve and forest plot. Enrichment analysis of Oncogenic Signaling Pathways was also performed to exhibit the difference between these two groups. Moreover, recent studies have demonstrated that a higher tumor mutated burden (TMB) was strongly associated with a better anti-tumor immune response [57], so we also compared the difference of TMB between HRPS- and LRPS-group. In addition, the distributions of PRS between different gene mutations were also compared and visualized through box plots.

Prediction of response to checkpoint blocking-up and drugs

To further probe whether HRPS-group can benefit from checkpoint blocking-up and potential drugs, possibility of response to immunotherapy was predicted using an algorithm reported previously, including dysfunction and exclusion of anti-tumor immune (TIDE) [58]. The predicted responses to drugs were done using the R package "oncoPredict" based on version 2 database of Genomics of Drug Sensitivity in Cancer [59]. Using PRS from ARGs signature, Pearson correlation analysis was used to scan the candidate drugs, which had a *P* value less than 0.001 and correlation coefficient less than -0.3. Correlation coefficients reflected the relations between PRS and IC50 of candidate therapeutic agents. And then the differences of candidate agents were also compared between HRPS- and LRPS-group.

Construction of a nomogram using 7-ARGs signature

To appraise clinical applicability, we established a nomogram using variables with independent prognostic

values in multivariable analysis of COX proportional hazards regression model in the training set. Variance inflation factor (VIF) was calculated to test the collinearity among predictors, and variables with a VIF value less than 5 were excluded from collinearity. Curves of C-statistic and calibration were draw to demonstrate the efficacy and accuracy of nomogram, while decision curve analysis (DCA) was executed for evaluation of clinical utility.

Statistical settings

Statistical processes were conducted by related packages of R 4.1 software. Tests of Fisher exact/Chi-square were run to analyse categorical variables, whereas tests of Kruskal-Wallis/Wilcoxon rank-sum were done for numerical variables. Curves of Kaplan-Meier with test of Log-rank/COX analysis were utilized to estimate the difference of overall survival (OS). When the values of P less than a threshold (< 0.05), the results were deemed to be statistically different.

AUTHOR CONTRIBUTIONS

Conceptualization and design: Suning Chen and Xiebing Bao; Data acquisition: Peng Ke, Qian Zhu and Ting Xu; Methodology: Peng Ke, Qian Zhu, Ting Xu, Xiaofei Yang, Ying Wang, HuiYing Qiu, Depei Wu, Xiebing Bao and Suning Chen; Data analysis and interpretation: Suning Chen and Xiebing Bao; Writing (original draft): Peng Ke, Qian Zhu and Ting Xu; Writing (review and editing): Suning Chen and Xiebing Bao; Project administration: Suning Chen and Xiebing Bao.

ACKNOWLEDGMENTS

CONFLICTS OF INTEREST

All authors declared no relevant conflicts.

FUNDING

REFERENCES

1. Kelly LM, Gilliland DG. Genetics of myeloid leukemias. Annu Rev Genomics Hum Genet. 2002; 3:179–98. https://doi.org/10.1146/annurev.genom.3.032802.115046 PMID:12194988

2. Almeida AM, Ramos F. Acute myeloid leukemia in the older adults. Leuk Res Rep. 2016; 6:1–7. https://doi.org/10.1016/j.lrr.2016.06.001 PMID:27408788

3. Alibhai SM, Leach M, Minden MD, Brandwein J. Outcomes and quality of care in acute myeloid leukemia over 40 years. Cancer. 2009; 115:2903–11. https://doi.org/10.1002/cncr.24373 PMID:19452536

4. DiNardo CD, Pratz K, Pullarkat V, Jonas BA, Arellano M, Becker PS, Frankfurt O, Konopleva M, Wei AH, Kantarjian HM, Xu T, Hong WJ, Chyla B, et al. Venetoclax combined with decitabine or azacitidine in treatment-naive, elderly patients with acute myeloid leukemia. Blood. 2019; 133:7–17. https://doi.org/10.1182/blood-2018-08-868752 PMID:30361262

5. Dombret H, Seymour JF, Butrym A, Wierzbowska A, Selleslag D, Jang JH, Kumar R, Cavenagh J, Schuh AC, Candoni A, Récher C, Sandhu I, Bernal del Castillo T, et al. International phase 3 study of azacitidine vs conventional care regimens in older patients with newly diagnosed AML with >30% blasts. Blood. 2015; 126:291–9. https://doi.org/10.1182/blood-2015-01-621664 PMID:25987659

6. Mohammadi M, Cao Y, Glimelius I, Bottai M, Eloranta S, Smedby KE. The impact of comorbid disease history on all-cause and cancer-specific mortality in myeloid leukemia and myeloma - a Swedish population-based study. BMC Cancer. 2015; 15:850. https://doi.org/10.1186/s12885-015-1857-x PMID:26537111

7. Menzin J, Lang K, Earle CC, Kerney D, Mallick R. The outcomes and costs of acute myeloid leukemia among the elderly. Arch Intern Med. 2002; 162:1597–603. https://doi.org/10.1001/archinte.162.14.1597 PMID:12123403

8. Leith CP, Kopecky KJ, Godwin J, McConnell T, Slovak ML, Chen IM, Head DR, Appelbaum FR, Willman CL. Acute myeloid leukemia in the elderly: assessment of multidrug resistance (MDR1) and cytogenetics distinguishes biologic subgroups with remarkably distinct responses to standard chemotherapy. A Southwest Oncology Group study. Blood. 1997; 89:3323–9. PMID:9129038

9. Kennedy BK, Berger SL, Brunet A, Campisi J, Cuervo AM, Epel ES, Franceschi C, Lithgow GJ, Morimoto RI, Pessin JE, Rando TA, Richardson A, Schadt EE, et al.

Geroscience: linking aging to chronic disease. Cell. 2014; 159:709–13.
https://doi.org/10.1016/j.cell.2014.10.039
PMID:25417146

10. López-Otín C, Blasco MA, Partridge L, Serrano M, Kroemer G. The hallmarks of aging. Cell. 2013; 153:1194–217.
https://doi.org/10.1016/j.cell.2013.05.039
PMID:23746838

11. Rao AV, Valk PJ, Metzeler KH, Acharya CR, Tuchman SA, Stevenson MM, Rizzieri DA, Delwel R, Buske C, Bohlander SK, Potti A, Löwenberg B. Age-specific differences in oncogenic pathway dysregulation and anthracycline sensitivity in patients with acute myeloid leukemia. J Clin Oncol. 2009; 27:5580–6.
https://doi.org/10.1200/JCO.2009.22.2547
PMID:19858393

12. Abdel-Wahab O, Levine RL. Mutations in epigenetic modifiers in the pathogenesis and therapy of acute myeloid leukemia. Blood. 2013; 121:3563–72.
https://doi.org/10.1182/blood-2013-01-451781
PMID:23640996

13. Gibson KL, Wu YC, Barnett Y, Duggan O, Vaughan R, Kondeatis E, Nilsson BO, Wikby A, Kipling D, Dunn-Walters DK. B-cell diversity decreases in old age and is correlated with poor health status. Aging Cell. 2009; 8:18–25.
https://doi.org/10.1111/j.1474-9726.2008.00443.x
PMID:18986373

14. Wang B, Tong F, Zhai C, Wang L, Liu Y, Wang J. Derivation and Comprehensive Analysis of Aging Patterns in Patients with Bladder Cancer. Dis Markers. 2021; 2021:3385058.
https://doi.org/10.1155/2021/3385058
PMID:34721733

15. Luo C, Nie H, Yu L. Identification of Aging-Related Genes Associated with Prognostic Value and Immune Microenvironment Characteristics in Diffuse Large B-Cell Lymphoma. Oxid Med Cell Longev. 2022; 2022:3334522.
https://doi.org/10.1155/2022/3334522
PMID:35069971

16. Chen X, Wang L, Hong L, Su Z, Zhong X, Zhou H, Zhang X, Wu J, Shao L. Identification of Aging-Related Genes Associated With Clinical and Prognostic Features of Hepatocellular Carcinoma. Front Genet. 2021; 12:661988.
https://doi.org/10.3389/fgene.2021.661988
PMID:34262594

17. Yue T, Chen S, Zhu J, Guo S, Huang Z, Wang P, Zuo S, Liu Y. The aging-related risk signature in colorectal cancer. Aging (Albany NY). 2021; 13:7330–49.
https://doi.org/10.18632/aging.202589
PMID:33658390

18. Mahmoudi S, Xu L, Brunet A. Turning back time with emerging rejuvenation strategies. Nat Cell Biol. 2019; 21:32–43.
https://doi.org/10.1038/s41556-018-0206-0
PMID:30602763

19. Tacutu R, Thornton D, Johnson E, Budovsky A, Barardo D, Craig T, Diana E, Lehmann G, Toren D, Wang J, Fraifeld VE, de Magalhães JP. Human Ageing Genomic Resources: new and updated databases. Nucleic Acids Res. 2018; 46:D1083–90.
https://doi.org/10.1093/nar/gkx1042 PMID:29121237

20. Ishwaran H, Kogalur UB. Consistency of Random Survival Forests. Stat Probab Lett. 2010; 80:1056–64.
https://doi.org/10.1016/j.spl.2010.02.020
PMID:20582150

21. Lerch E, Espeli V, Zucca E, Leoncini L, Scali G, Mora O, Bordoni A, Cavalli F, Ghielmini M. Prognosis of acute myeloid leukemia in the general population: data from southern Switzerland. Tumori. 2009.
https://doi.org/10.1177/030089160909500306
PMID:19688968

22. Prenkert M, Uggla B, Tina E, Tidefelt U, Strid H. Rapid induction of P-glycoprotein mRNA and protein expression by cytarabine in HL-60 cells. Anticancer Res. 2009; 29:4071–6.
PMID:19846953

23. Hezel AF, Bardeesy N. LKB1; linking cell structure and tumor suppression. Oncogene. 2008; 27:6908–19.
https://doi.org/10.1038/onc.2008.342 PMID:19029933

24. Green AS, Chapuis N, Maciel TT, Willems L, Lambert M, Arnoult C, Boyer O, Bardet V, Park S, Foretz M, Viollet B, Ifrah N, Dreyfus F, et al. The LKB1/AMPK signaling pathway has tumor suppressor activity in acute myeloid leukemia through the repression of mTOR-dependent oncogenic mRNA translation. Blood. 2010; 116:4262–73.
https://doi.org/10.1182/blood-2010-02-269837
PMID:20668229

25. Huang S, Zhang B, Fan W, Zhao Q, Yang L, Xin W, Fu D. Identification of prognostic genes in the acute myeloid leukemia microenvironment. Aging (Albany NY). 2019; 11:10557–80.
https://doi.org/10.18632/aging.102477
PMID:31740623

26. Mantovani A, Allavena P, Sica A, Balkwill F. Cancer-related inflammation. Nature. 2008; 454:436–44.
https://doi.org/10.1038/nature07205
PMID:18650914

27. Rhodes CA, Dougherty PG, Cooper JK, Qian Z, Lindert S, Wang QE, Pei D. Cell-Permeable Bicyclic Peptidyl Inhibitors against NEMO-IκB Kinase Interaction Directly from a Combinatorial Library. J Am Chem Soc. 2018; 140:12102–10.
https://doi.org/10.1021/jacs.8b06738
PMID:30176143

28. Guzman ML, Swiderski CF, Howard DS, Grimes BA, Rossi RM, Szilvassy SJ, Jordan CT. Preferential induction of apoptosis for primary human leukemic stem cells. Proc Natl Acad Sci USA. 2002; 99:16220–5.
https://doi.org/10.1073/pnas.252462599
PMID:12451177

29. Baumgartner B, Weber M, Quirling M, Fischer C, Page S, Adam M, Von Schilling C, Waterhouse C, Schmid C, Neumeier D, Brand K. Increased IkappaB kinase activity is associated with activated NF-kappaB in acute myeloid blasts. Leukemia. 2002; 16:2062–71.
https://doi.org/10.1038/sj.leu.2402641
PMID:12357358

30. Birkenkamp KU, Geugien M, Schepers H, Westra J, Lemmink HH, Vellenga E. Constitutive NF-kappaB DNA-binding activity in AML is frequently mediated by a Ras/PI3-K/PKB-dependent pathway. Leukemia. 2004; 18:103–12.
https://doi.org/10.1038/sj.leu.2403145
PMID:14574326

31. Guzman ML, Neering SJ, Upchurch D, Grimes B, Howard DS, Rizzieri DA, Luger SM, Jordan CT. Nuclear factor-kappaB is constitutively activated in primitive human acute myelogenous leukemia cells. Blood. 2001; 98:2301–7.
https://doi.org/10.1182/blood.v98.8.2301
PMID:11588023

32. Frelin C, Imbert V, Griessinger E, Peyron AC, Rochet N, Philip P, Dageville C, Sirvent A, Hummelsberger M, Bérard E, Dreano M, Sirvent N, Peyron JF. Targeting NF-kappaB activation via pharmacologic inhibition of IKK2-induced apoptosis of human acute myeloid leukemia cells. Blood. 2005; 105:804–11.
https://doi.org/10.1182/blood-2004-04-1463
PMID:15454494

33. Bosman MC, Schuringa JJ, Vellenga E. Constitutive NF-κB activation in AML: Causes and treatment strategies. Crit Rev Oncol Hematol. 2016; 98:35–44.
https://doi.org/10.1016/j.critrevonc.2015.10.001
PMID:26490297

34. Fröhling S, Scholl C, Gilliland DG, Levine RL. Genetics of myeloid malignancies: pathogenetic and clinical implications. J Clin Oncol. 2005; 23:6285–95.
https://doi.org/10.1200/JCO.2005.05.010
PMID:16155011

35. Kuilman T, Michaloglou C, Vredeveld LC, Douma S, van Doorn R, Desmet CJ, Aarden LA, Mooi WJ, Peeper DS. Oncogene-induced senescence relayed by an interleukin-dependent inflammatory network. Cell. 2008; 133:1019–31.
https://doi.org/10.1016/j.cell.2008.03.039
PMID:18555778

36. Yan H, Qu J, Cao W, Liu Y, Zheng G, Zhang E, Cai Z. Identification of prognostic genes in the acute myeloid leukemia immune microenvironment based on TCGA data analysis. Cancer Immunol Immunother. 2019; 68:1971–8.
https://doi.org/10.1007/s00262-019-02408-7
PMID:31650199

37. Gao L, Yu S, Zhang X. Hypothesis: Tim-3/galectin-9, a new pathway for leukemia stem cells survival by promoting expansion of myeloid-derived suppressor cells and differentiating into tumor-associated macrophages. Cell Biochem Biophys. 2014; 70:273–7.
https://doi.org/10.1007/s12013-014-9900-0
PMID:24639110

38. Yang X, Feng W, Wang R, Yang F, Wang L, Chen S, Ru Y, Cheng T, Zheng G. Repolarizing heterogeneous leukemia-associated macrophages with more M1 characteristics eliminates their pro-leukemic effects. Oncoimmunology. 2017; 7:e1412910.
https://doi.org/10.1080/2162402X.2017.1412910
PMID:29632729

39. Grauers Wiktorin H, Nilsson MS, Kiffin R, Sander FE, Lenox B, Rydström A, Hellstrand K, Martner A. Histamine targets myeloid-derived suppressor cells and improves the anti-tumor efficacy of PD-1/PD-L1 checkpoint blockade. Cancer Immunol Immunother. 2019; 68:163–74.
https://doi.org/10.1007/s00262-018-2253-6
PMID:30315349

40. Lian J, Yue Y, Yu W, Zhang Y. Immunosenescence: a key player in cancer development. J Hematol Oncol. 2020; 13:151.
https://doi.org/10.1186/s13045-020-00986-z
PMID:33168037

41. Johnson ND, Conneely KN. The role of DNA methylation and hydroxymethylation in immunosenescence. Ageing Res Rev. 2019; 51:11–23.
https://doi.org/10.1016/j.arr.2019.01.011
PMID:30769150

42. Topalian SL, Taube JM, Anders RA, Pardoll DM. Mechanism-driven biomarkers to guide immune checkpoint blockade in cancer therapy. Nat Rev Cancer. 2016; 16:275–87.
https://doi.org/10.1038/nrc.2016.36
PMID:27079802

43. Ravandi F, Assi R, Daver N, Benton CB, Kadia T, Thompson PA, Borthakur G, Alvarado Y, Jabbour EJ, Konopleva M, Takahashi K, Kornblau S, DiNardo CD, et al. Idarubicin, cytarabine, and nivolumab in patients with newly diagnosed acute myeloid leukaemia or high-risk myelodysplastic syndrome: a single-arm, phase 2 study. Lancet Haematol. 2019; 6:e480–8.
https://doi.org/10.1016/S2352-3026(19)30114-0
PMID:31400961

44. Daver N, Garcia-Manero G, Basu S, Boddu PC, Alfayez M, Cortes JE, Konopleva M, Ravandi-Kashani F, Jabbour E, Kadia T, Nogueras-Gonzalez GM, Ning J, Pemmaraju N, et al. Efficacy, Safety, and Biomarkers of Response to Azacitidine and Nivolumab in Relapsed/Refractory Acute Myeloid Leukemia: A Nonrandomized, Open-Label, Phase II Study. Cancer Discov. 2019; 9:370–83.
https://doi.org/10.1158/2159-8290.CD-18-0774
PMID:30409776

45. Kong T, Laranjeira AB, Collins TB, De Togni ES, Wong AJ, Fulbright MC, Ruzinova M, Celik H, Challen GA, Fisher DA, Oh ST. Pevonedistat targets malignant cells in myeloproliferative neoplasms *in vitro* and *in vivo* via NFκB pathway inhibition. Blood Adv. 2022; 6:611–23.
https://doi.org/10.1182/bloodadvances.2020002804
PMID:34644371

46. Fontana L, Partridge L, Longo VD. Extending healthy life span--from yeast to humans. Science. 2010; 328:321–6.
https://doi.org/10.1126/science.1172539
PMID:20395504

47. Yanada M, Yamamoto Y, Iba S, Okamoto A, Inaguma Y, Tokuda M, Morishima S, Kanie T, Mizuta S, Akatsuka Y, Okamoto M, Emi N. TP53 mutations in older adults with acute myeloid leukemia. Int J Hematol. 2016; 103:429–35.
https://doi.org/10.1007/s12185-016-1942-1
PMID:26781615

48. Wang C, Ding Y, Liu Y, Zhang Q, Xu S, Xia L, Duan H, Wang S, Ji P, Huang W, Zhao G, Cao Z, Shen H, Wang Y. Identification of Mutated Peptides in Bladder Cancer From Exomic Sequencing Data Reveals Negative Correlation Between Mutation-Specific Immunoreactivity and Inflammation. Front Immunol. 2020; 11:576603.
https://doi.org/10.3389/fimmu.2020.576603
PMID:33329543

49. Ibrahimpasic T, Ghossein R, Shah JP, Ganly I. Poorly Differentiated Carcinoma of the Thyroid Gland: Current Status and Future Prospects. Thyroid. 2019; 29:311–21.
https://doi.org/10.1089/thy.2018.0509
PMID:30747050

50. Shao Y, Hu X, Yang Z, Lia T, Yang W, Wu K, Ren S, Xiong S, Dou W, Feng S, Wang Y, Liu Y, Wu K, Li X. Prognostic factors of non-muscle invasive bladder cancer: a study based on next-generation sequencing. Cancer Cell Int. 2021; 21:23.
https://doi.org/10.1186/s12935-020-01731-9
PMID:33407469

51. Qing T, Zhu S, Suo C, Zhang L, Zheng Y, Shi L. Somatic mutations in ZFHX4 gene are associated with poor overall survival of Chinese esophageal squamous cell carcinoma patients. Sci Rep. 2017; 7:4951.
https://doi.org/10.1038/s41598-017-04221-7
PMID:28694483

52. Rosenwald A, Bens S, Advani R, Barrans S, Copie-Bergman C, Elsensohn MH, Natkunam Y, Calaminici M, Sander B, Baia M, Smith A, Painter D, Pham L, et al. Prognostic Significance of *MYC* Rearrangement and Translocation Partner in Diffuse Large B-Cell Lymphoma: A Study by the Lunenburg Lymphoma Biomarker Consortium. J Clin Oncol. 2019; 37:3359–68.
https://doi.org/10.1200/JCO.19.00743
PMID:31498031

53. Charoentong P, Finotello F, Angelova M, Mayer C, Efremova M, Rieder D, Hackl H, Trajanoski Z. Pan-cancer Immunogenomic Analyses Reveal Genotype-Immunophenotype Relationships and Predictors of Response to Checkpoint Blockade. Cell Rep. 2017; 18:248–62.
https://doi.org/10.1016/j.celrep.2016.12.019
PMID:28052254

54. Ding C, Shan Z, Li M, Chen H, Li X, Jin Z. Characterization of the fatty acid metabolism in colorectal cancer to guide clinical therapy. Mol Ther Oncolytics. 2021; 20:532–44.
https://doi.org/10.1016/j.omto.2021.02.010
PMID:33738339

55. Hanahan D, Weinberg RA. Hallmarks of cancer: the next generation. Cell. 2011; 144:646–74.
https://doi.org/10.1016/j.cell.2011.02.013
PMID:21376230

56. Mayakonda A, Lin DC, Assenov Y, Plass C, Koeffler HP. Maftools: efficient and comprehensive analysis of somatic variants in cancer. Genome Res. 2018; 28:1747–56.
https://doi.org/10.1101/gr.239244.118
PMID:30341162

57. Robinson DR, Wu YM, Lonigro RJ, Vats P, Cobain E, Everett J, Cao X, Rabban E, Kumar-Sinha C, Raymond V, Schuetze S, Alva A, Siddiqui J, et al. Integrative clinical genomics of metastatic cancer. Nature. 2017; 548:297–303.
https://doi.org/10.1038/nature23306
PMID:28783718

58. Jiang P, Gu S, Pan D, Fu J, Sahu A, Hu X, Li Z, Traugh N, Bu X, Li B, Liu J, Freeman GJ, Brown MA, et al. Signatures of T cell dysfunction and exclusion predict cancer immunotherapy response. Nat Med. 2018; 24:1550–8.
https://doi.org/10.1038/s41591-018-0136-1
PMID:30127393

59. Maeser D, Gruener RF, Huang RS. oncoPredict: an R package for predicting *in vivo* or cancer patient drug response and biomarkers from cell line screening data. Brief Bioinform. 2021; 22:bbab260.
https://doi.org/10.1093/bib/bbab260
PMID:34260682

Supplementary Figures
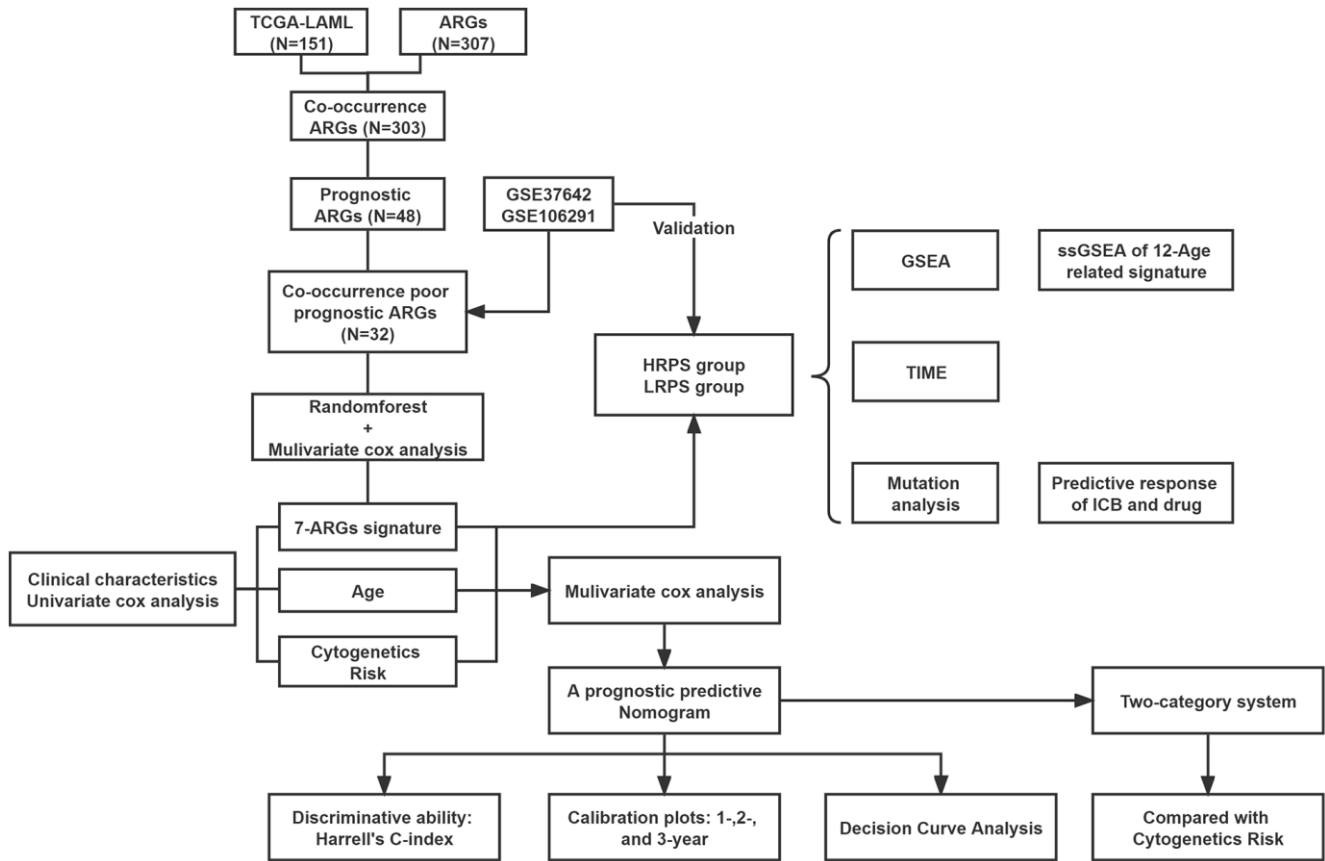
Supplementary Figure 1. Work flow of the current study. ARGs indicated aging-related genes. TIME indicated immune microenvironment of tumor.

Gene	HR (95% CI)		P-value
PDGFRA	1.932(1.25−2.986)		0.003
LEP	1.826(1.193−2.796)		0.006
HBP1	1.712(1.115−2.628)		0.014
GHR	1.699(1.108−2.606)		0.015
AR	1.678(1.096−2.569)		0.017
EGFR	1.676(1.094−2.568)		0.018
TPP2	1.668(1.085−2.563)		0.02
MXD1	1.633(1.063−2.51)		0.025
INSR	1.623(1.061−2.484)		0.026
IGF2	1.615(1.057−2.467)		0.027
IGFBP3	1.605(1.049−2.455)		0.029
PIK3CB	1.576(1.028−2.418)		0.037
IGF1R	1.542(1.008−2.358)		0.046
BMI1	0.647(0.423−0.989)		0.044
GCLM	0.646(0.422−0.987)		0.043
MT1E	0.642(0.418−0.987)		0.043
MAP3K5	0.633(0.413−0.969)		0.035
SPRTN	0.631(0.411−0.971)		0.036
PTK2B	0.631(0.412−0.966)		0.034
UCP3	0.625(0.41−0.955)		0.03
PRDX1	0.618(0.404−0.944)		0.026
DGAT1	0.618(0.404−0.945)		0.026
ERCC2	0.617(0.403−0.944)		0.026
PRKCD	0.611(0.399−0.936)		0.024
EMD	0.608(0.398−0.928)		0.021
HSPA1A	0.603(0.393−0.924)		0.02
NFKB2	0.6(0.393−0.918)		0.019
SOD1	0.594(0.388−0.908)		0.016
SOCS2	0.589(0.385−0.9)		0.014
STK11	0.576(0.375−0.886)		0.012
GSK3A	0.576(0.377−0.881)		0.011
GSTP1	0.565(0.369−0.865)		0.009
GPX4	0.561(0.365−0.862)		0.008
HDAC3	0.559(0.365−0.857)		0.008
ERCC1	0.549(0.358−0.843)		0.006
PPP1CA	0.546(0.357−0.834)		0.005
TRAP1	0.545(0.356−0.835)		0.005
ELN	0.532(0.346−0.819)		0.004
NUDT1	0.519(0.339−0.795)		0.003
TGFB1	0.51(0.331−0.785)		0.002
TERF2	0.5(0.326−0.766)		0.001
BAK1	0.493(0.321−0.756)		0.001
SIRT6	0.486(0.317−0.746)		0.001
GPX1	0.478(0.31−0.735)		0.001
UCP2	0.473(0.308−0.728)		0.001
PTPN1	0.458(0.297−0.706)		<0.001
HSPA1B	0.43(0.277−0.666)		<0.001
LMNA	0.429(0.277−0.665)		<0.001

Hazard Ratio: 0.5 1 1.5 2 2.5 3

Supplementary Figure 2. Prognostic analyses of 84 ARGs in training cohort. Median expression values of genes were used as the threshold values, and patients with high value than which were set as a reference group.
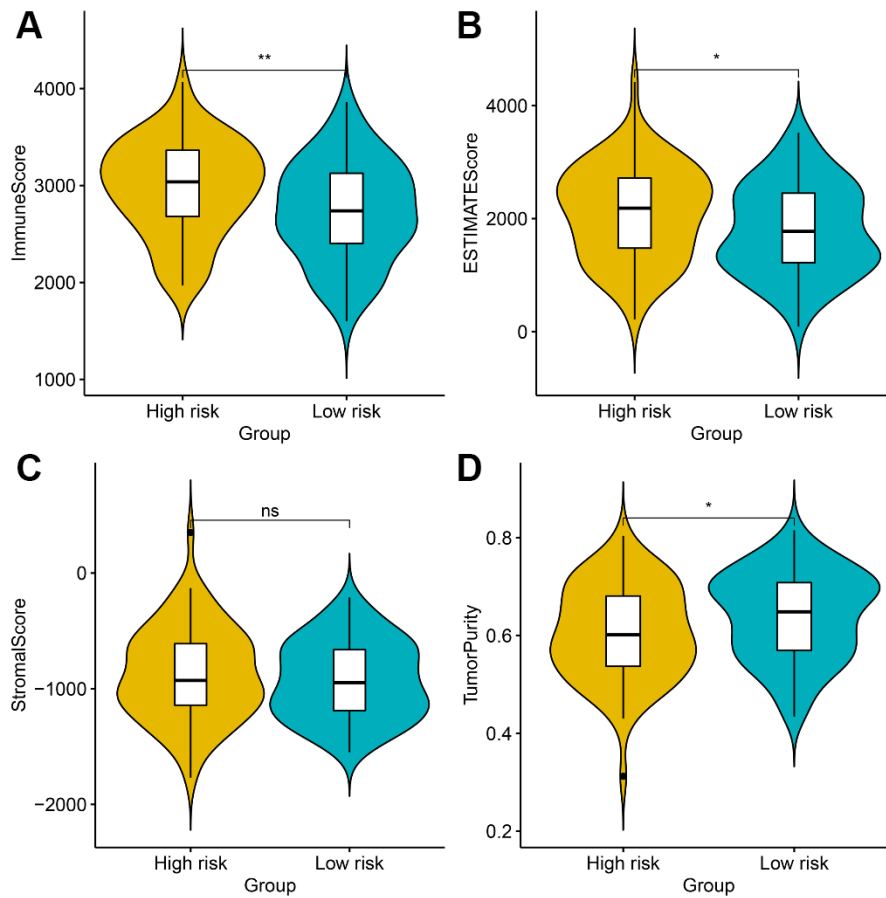
Supplementary Figure 3. Characteristics of immune-related microenvironment in HRPS-group/high-risk group and LRPS-group/low-risk group. (**A**) Immune Scores. (**B**) ESTIMATE Scores. (**C**) Stromal scores. (**D**) Tumor Purity. (*P < 0.05, **P <0.01, ***P < 0.001).
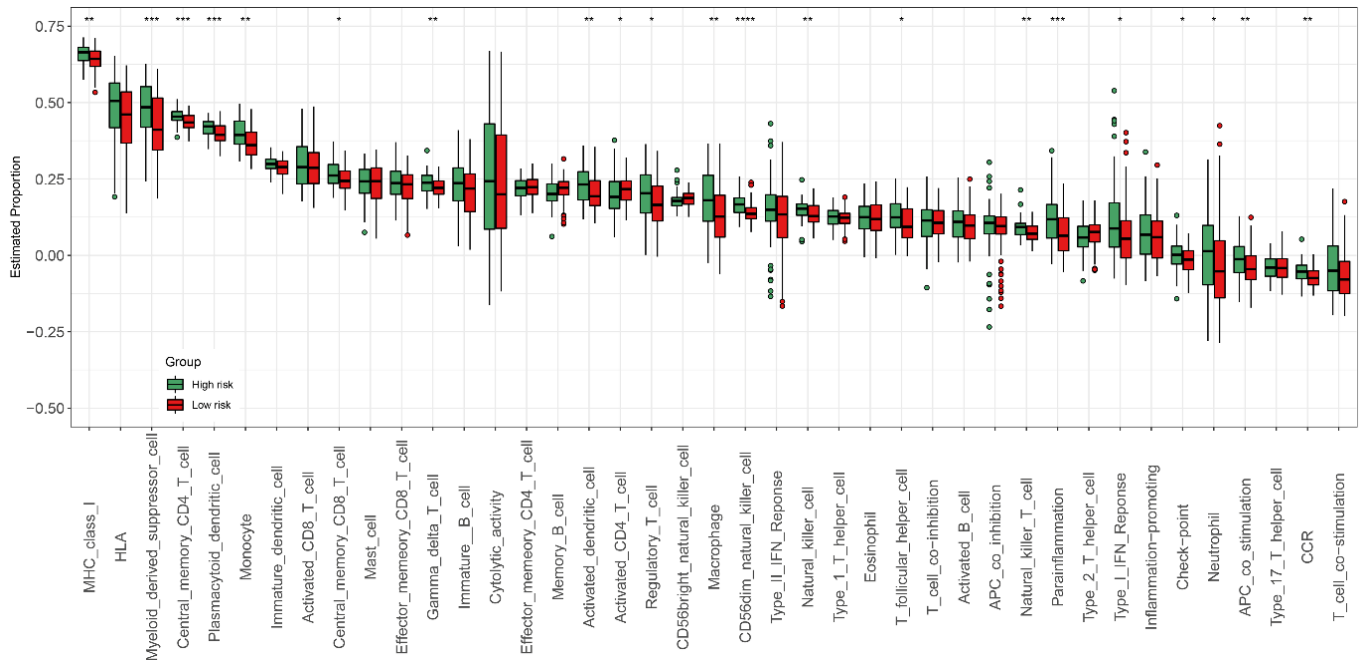
Supplementary Figure 4. Different cell abundance of forty-one immune categories between HRPS-group/high-risk group and LRPS-group/low-risk group. (*P < 0.05, **P <0.01, ***P < 0.001).
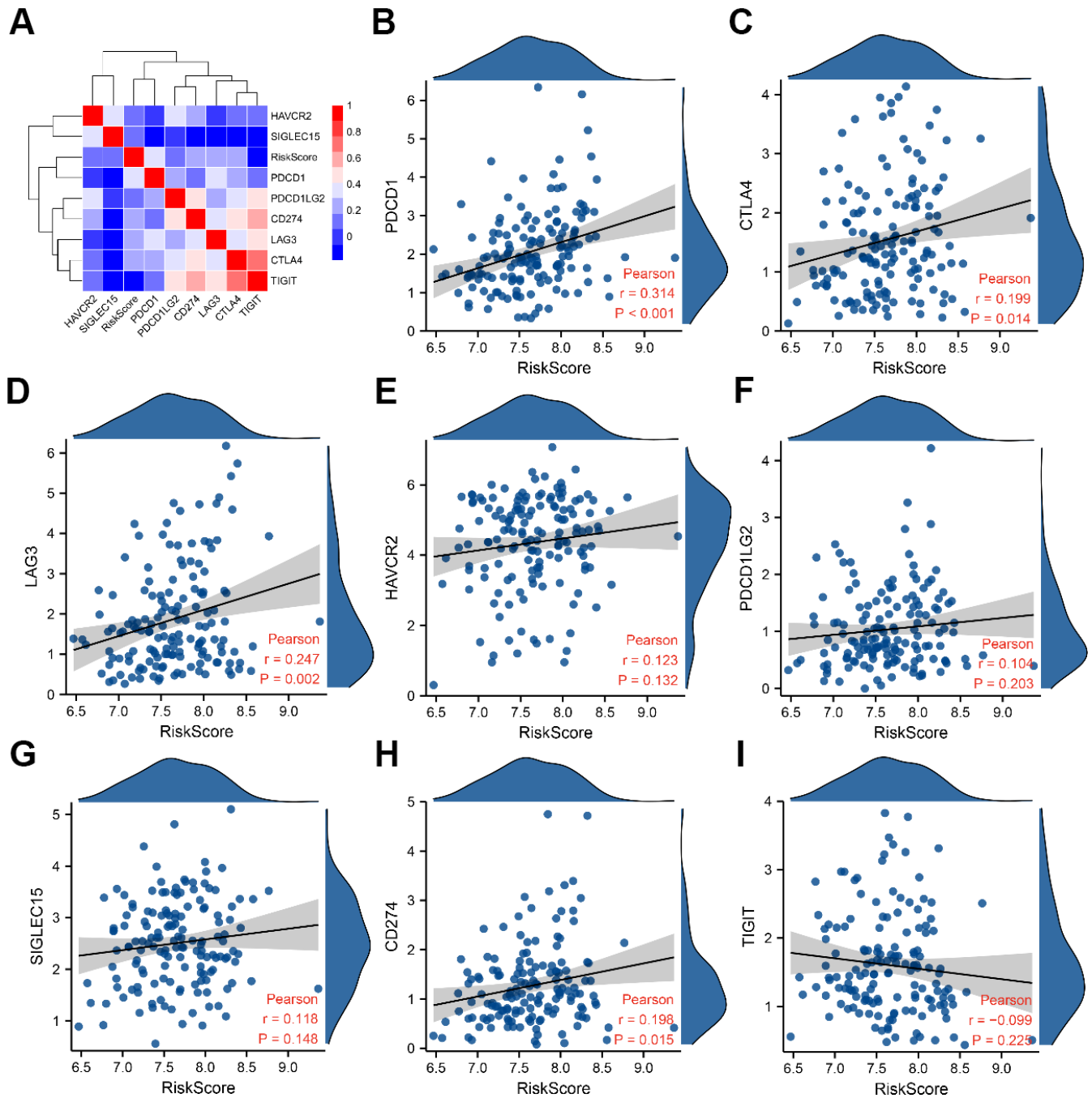
Supplementary Figure 5. Relationship between PRS and 8 checkpoints' expression. (**A**) The heatmap of correlation between PRS score and 8 immune checkpoint expression levels. (**B**–**I**) Scatter plot of correlation between PRS score and expression level of each immune checkpoint.
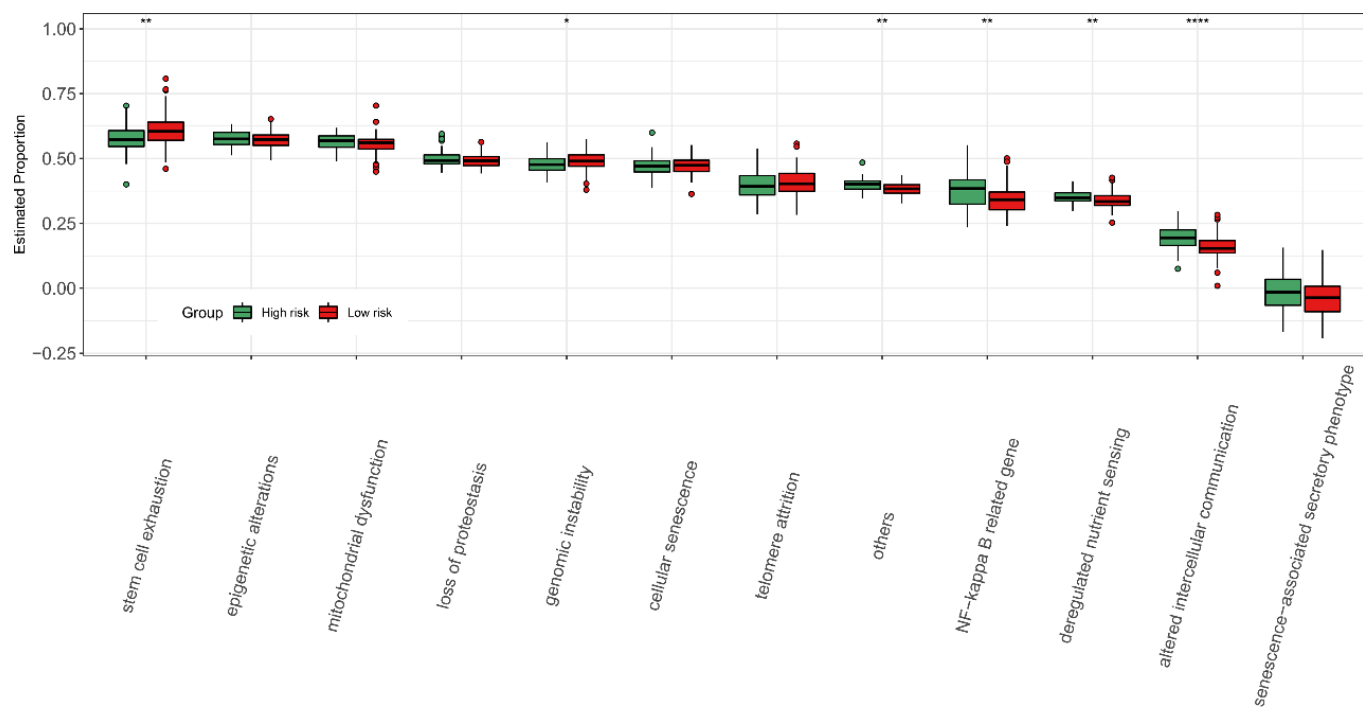
Supplementary Figure 6. Difference of ssGSEA scores about 12 aging-related gene signals between two different PRS groups according to ARGs prognostic signature. (*P < 0.05, **P <0.01, ***P < 0.001).
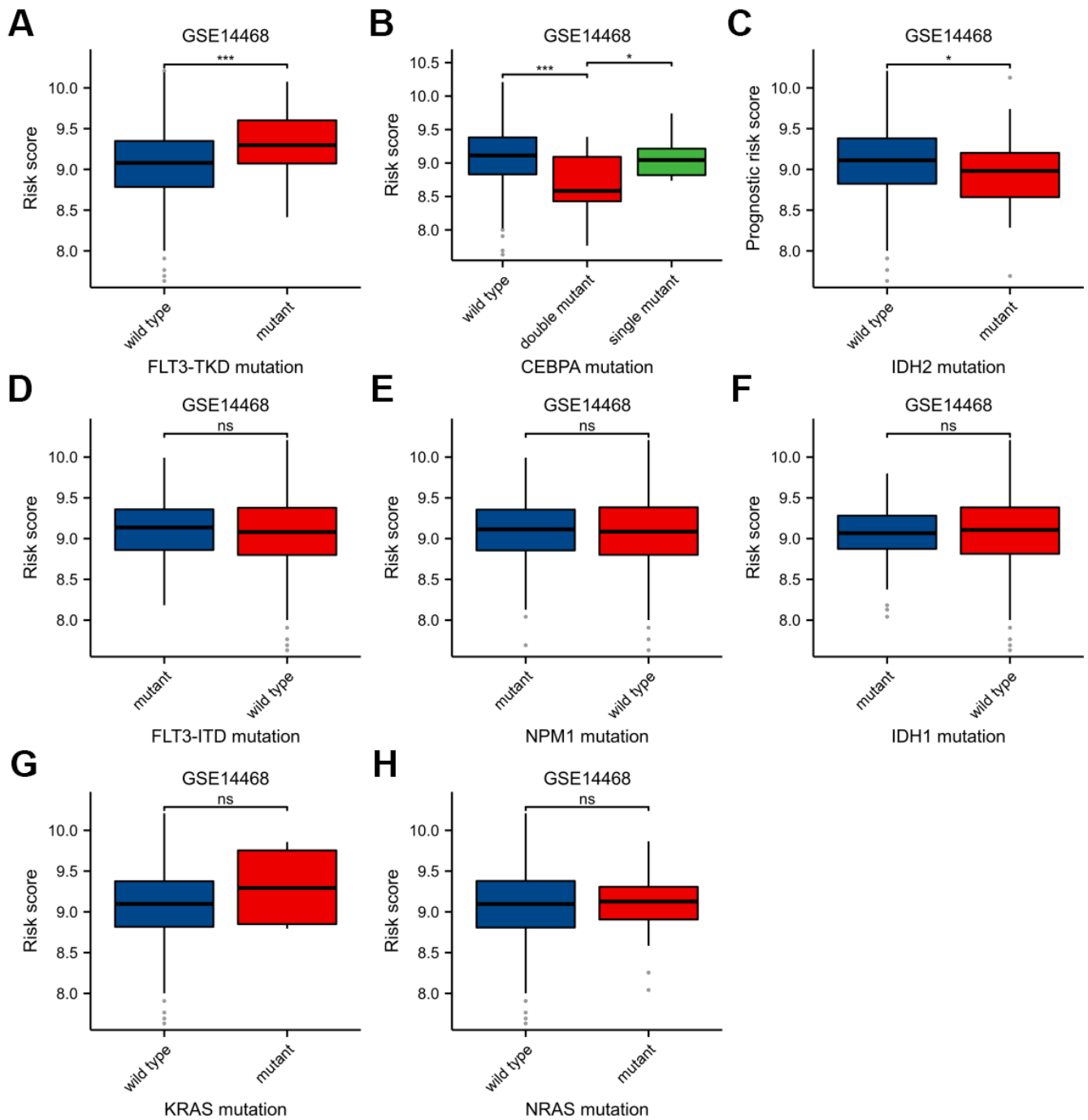
Supplementary Figure 7. Differences of PRS between wild-type and mutation of several common genes. (**A**) *FLT3-TKD,* (**B**) *CEBPA*, (**C**) *IDH2*, (**D**) *FLT3-ITD*, (**E**) *NPM*1, (**F**) *IDH1*, (**G**) *KRAS*, (**H**) *NRAS*. (*P < 0.05, **P <0.01, ***P < 0.001).

Supplementary Tables

Please browse Full Text version to see the data of Supplementary Tables 1, 2, 4–6, 8.

Supplementary Table 1. Three hundred seven human genes related to aging.

Supplementary Table 2. Univariate analyses of 303 ARGs for overall survival.

Supplementary Table 3. 48 ARGs were associated with prognosis by univariate analyses.

Gene name	Coef	Se	P	HR	95%CI low	95%CI High
LMNA	-0.845	0.223	<0.001	0.429	0.277	0.665
HSPA1B	-0.844	0.224	<0.001	0.430	0.277	0.666
PTPN1	-0.780	0.221	<0.001	0.458	0.297	0.706
UCP2	-0.748	0.220	0.001	0.473	0.308	0.728
GPX1	-0.739	0.220	0.001	0.478	0.310	0.735
SIRT6	-0.721	0.218	0.001	0.486	0.317	0.746
BAK1	-0.708	0.218	0.001	0.493	0.321	0.756
TERF2	-0.694	0.218	0.001	0.500	0.326	0.766
TGFB1	-0.673	0.220	0.002	0.510	0.331	0.785
NUDT1	-0.656	0.218	0.003	0.519	0.339	0.795
ELN	-0.631	0.220	0.004	0.532	0.346	0.819
TRAP1	-0.606	0.217	0.005	0.545	0.356	0.835
PPP1CA	-0.606	0.217	0.005	0.546	0.357	0.834
ERCC1	-0.599	0.218	0.006	0.549	0.358	0.843
HDAC3	-0.581	0.218	0.008	0.559	0.365	0.857
GPX4	-0.578	0.219	0.008	0.561	0.365	0.862
GSTP1	-0.571	0.218	0.009	0.565	0.369	0.865
STK11	-0.551	0.219	0.012	0.576	0.375	0.886
GSK3A	-0.551	0.217	0.011	0.576	0.377	0.881
SOCS2	-0.530	0.216	0.014	0.589	0.385	0.900
SOD1	-0.521	0.217	0.016	0.594	0.388	0.908
NFKB2	-0.510	0.217	0.019	0.600	0.393	0.918
HSPA1A	-0.506	0.218	0.020	0.603	0.393	0.924
EMD	-0.498	0.216	0.021	0.608	0.398	0.928
PRKCD	-0.492	0.218	0.024	0.611	0.399	0.936
ERCC2	-0.483	0.217	0.026	0.617	0.403	0.944
PRDX1	-0.482	0.216	0.026	0.618	0.404	0.944
DGAT1	-0.481	0.217	0.026	0.618	0.404	0.945
UCP3	-0.470	0.216	0.030	0.625	0.410	0.955
SPRTN	-0.460	0.219	0.036	0.631	0.411	0.971
PTK2B	-0.461	0.217	0.034	0.631	0.412	0.966
MAP3K5	-0.458	0.218	0.035	0.633	0.413	0.969
MT1E	-0.443	0.219	0.043	0.642	0.418	0.987
GCLM	-0.437	0.217	0.043	0.646	0.422	0.987
BMI1	-0.435	0.217	0.044	0.647	0.423	0.989
IGF1R	0.433	0.217	0.046	1.542	1.008	2.358
PIK3CB	0.455	0.218	0.037	1.576	1.028	2.418
IGFBP3	0.473	0.217	0.029	1.605	1.049	2.455
IGF2	0.479	0.216	0.027	1.615	1.057	2.467
INSR	0.484	0.217	0.026	1.623	1.061	2.484
MXD1	0.491	0.219	0.025	1.633	1.063	2.510

TPP2	0.511	0.219	0.020	1.668	1.085	2.563
EGFR	0.517	0.218	0.018	1.676	1.094	2.568
AR	0.518	0.217	0.017	1.678	1.096	2.569
GHR	0.530	0.218	0.015	1.699	1.108	2.606
HBP1	0.537	0.219	0.014	1.712	1.115	2.628
LEP	0.602	0.217	0.006	1.826	1.193	2.796
PDGFRA	0.659	0.222	0.003	1.932	1.250	2.986

Supplementary Table 4. List of pan-cancer immune metagenes.

Supplementary Table 5. Single-sample gene-set for tumor immune microenvironment analysis.

Supplementary Table 6. Twelve aging-related gene sets.

Supplementary Table 7. Pearson correlation analysis for scanning candidate therapeutic drugs.

Drug	Correlation coefficient	P value
Temozolomide_1375	-0.498212053	7.55E-11
PF-4708671_1129	-0.456825471	3.73E-09
Dactolisib_1057	-0.449715456	6.92E-09
5-Fluorouracil_1073	-0.433863895	2.62E-08
Entospletinib_1630	-0.431496025	3.18E-08
GNE-317_1926	-0.428702113	3.98E-08
Docetaxel_1007	-0.422628101	6.46E-08
Buparlisib_1873	-0.404751894	0.000000254
Pictilisib_1058	-0.401218856	0.00000033
VE821_2111	-0.398435368	0.000000405
MK-1775_1179	-0.384249796	0.00000111
AZD6738_1917	-0.383087068	0.0000012
Ribociclib_1632	-0.378656045	0.00000163
I-BRD9_1928	-0.378593752	0.00000164
Epirubicin_1511	-0.374221827	0.00000221
Axitinib_1021	-0.371145192	0.00000271
Bortezomib_1191	-0.366131208	0.00000378
YK-4-279_1239	-0.365077256	0.00000405
BDP-00009066_1866	-0.361748895	0.00000502
Camptothecin_1003	-0.357320265	0.00000667
Dabrafenib_1373	-0.351902382	0.00000938
BMS-345541_1249	-0.347824221	0.0000121
LGK974_1598	-0.347573101	0.0000123
Pevonedistat_1529	-0.346222958	0.0000133
Rapamycin_1084	-0.344928758	0.0000144
Luminespib_1559	-0.327708687	0.00004
BMS-536924_1091	-0.32390617	0.0000497
Leflunomide_1578	-0.321775903	0.000056
Wnt-C59_1622	-0.315870815	0.0000779
Dihydrorotenone_1827	-0.314568802	0.0000836
OTX015_1626	-0.31079521	0.000102746
Wee1 Inhibitor_1046	-0.309397471	0.000110801

Palbociclib_1054	-0.305193518	0.000138723
Ulixertinib_2047	-0.305018131	0.000140019
Taselisib_1561	-0.304662036	0.000142686
Sinularin_1838	-0.304160416	0.000146524
Vincristine_1818	-0.301715921	0.000166641

Supplementary Table 8. Predicted IC50 of candidate therapeutic drugs.

Supplementary Table 9. Univariate COX regression analysis for the overall survival.

Characteristics	Total (N)	Univariate analysis	
		Hazard ratio (95% CI)	P value
Risk Score	140	2.718 (1.810-4.081)	<0.001
Age	140	1.042 (1.026-1.058)	<0.001
Cytogenetics risk	138		
Favorable	31	1	
Intermediate	76	2.957 (1.498-5.836)	0.002
Poor	31	4.157 (1.944-8.893)	<0.001
PB-Blast (%)	140	1.003 (0.995-1.012)	0.445
BM-blast (%)	140	1.002 (0.995-1.009)	0.572
Hemoglobin (g/L)	139	1.117 (0.958-1.301)	0.157
WBC ($\times 10^9$/L)	139	1.005 (1.000-1.010)	0.069
PLT ($\times 10^9$/L)	140	1.000 (0.997-1.004)	0.842
Gender	140		
Male	77	1	
Female	63	0.971 (0.636-1.483)	0.892
Race	140		
White	127	1	
Others	10	1.154 (0.377-1.991)	0.736
FLT3 mutation	136		
Negative	97	1	
Positive	39	1.271 (0.801-2.016)	0.309
RAS mutation	139		
Negative	131	1	
Positive	8	0.643 (0.235-1.760)	0.39
NPM1 mutation	139		
Negative	106	1	
Positive	33	1.137 (0.706-1.832)	0.596
IDH1 mutation	138		
Negative	126	1	
Positive	12	0.588 (0.238-1.452)	0.249

Abbreviations: CI, confidence interval; FLT3, FMS-like tyrosine kinase 3; NPM1, Nucleophosmin; IDH1, Isocitrate dehydrogenase 1; PB, Peripheral blood; BM, Bone marrow; WBC, White blood cell; PLT, Platelet.